National Research FLAGSHIPS
Wealth from Oceans

CSIRO

Defining Regional Connections in Southwestern Pacific Swordfish

Chris Wilcox
FRDC Project 2007-036
May, 2014

www.csiro.au

FRDC
FISHERIES RESEARCH & DEVELOPMENT CORPORATION

Title: Defining regional connections in Southwestern Pacific Swordfish

Author: C. Wilcox

FRDC Project No: 2007/036

Published by: CSIRO Wealth from Oceans Flagship, 2014

ISBN: 978-0-643-10847-9

Suggested Citation
Wilcox, C. (2014) Defining Regional Connections in Southwestern Pacific Swordfish. FRDC Report 2007/036. CSIRO. Hobart, Australia. 74 pp.

Contents

List of Figures

List of Tables

1. NON TECHNICAL SUMMARY

2007/036: Defining regional connections in Southwestern Pacific broadbill swordfish

PRINCIPAL INVESTIGATOR: Chris Wilcox

ADDRESS: CSIRO Marine and Atmospheric Research
Castray Esplanade
Hobart, TAS 7000
Telephone (03) 6232 5306
Fax (03) 6232 5000

OBJECTIVES:

1. Collect Swordfish movement data and habitat preferences on the Coral Sea spawning grounds and during subsequent migration using electronic tags
2. Collate data from this study with data from ongoing studies on Swordfish movement in the Tasman Sea, east of New Zealand, and in the central South Pacific spawning area.
3. Refine existing analysis methods to incorporate electronic tag data and oscillatory movements such as annual migrations
4. Parameterize a regional movement model which describes retention times on the spawning grounds and migration patterns
5. Provide a succinct description of stock structure and movement that can be incorporated into other analyses.

NON TECHNICAL SUMMARY:

OUTCOMES ACHIEVED TO DATE

The project outputs have contributed to or will lead to the following outcomes:

1. Improved understanding of the connectivity between fish in the Tasman and Coral Seas fished by the Australian pelagic longline fishery and the Southwestern Pacific Swordfish stock.
2. Improved understanding of the movement and behavior of individual fish, in particular with respect to site fidelity by individual fish.

3. Increased capacity for management of phenomena such as spatial depletion, which depend on an understanding of stock mixing rates.
4. Improved basis for the design of future stock assessments for Swordfish in the Southwest Pacific region, in particular availability of project outputs that can be used to directly estimate mixing rates between locations.
5. Increased capacity for analysis of satellite tagging data for pelagic fishes, in particular for fish using satellite transmitting archival tags.
6. Indirect incorporation of tagging information into two regional stock assessments for Swordfish, via evaluation of mixing rates and likely stock structure.

The goal of this project was to investigate the distribution and movement of Swordfish in the Coral and Tasman Seas. At the time the project was funded the fishery was moving toward implementing spatial management, and was coping with a significant reduction in catch rates off the east coast of Australia. It was thought that this reduction was due to depletion of locally resident Swordfish. Although the serial declines in catch at various seamounts strongly pointed to local residence patterns, there was only a small amount of conventional tagging data available at the time to provide direct information on movement and site fidelity by Swordfish.

This project was composed of three parts, first 14 electronic tags were deployed on Swordfish to collect data on movement, second a statistical model of uncertainty in locations recovered from these electronic tags was developed, and third, a statistical model for analysing movement and residence patterns was developed and used to explore the new data collected on Swordfish. The project was significantly delayed by the collapse in Swordfish targeting approximately 6 months after the project was funded. Despite the long delay that this caused, the data was collected and the analysis completed as proposed.

Tagging operations were conducted from commercial fishing vessels operating between 154°E and 160°E and 24°S and 29.5°S. During the project CSIRO assisted in the development of a new towed electronic tag incorporating a GPS sensor, which significantly increased the quality of the data available. Using these tags and improved deployment methods, the project was able to obtain 277 position estimates across the 14 tagged fish. Tagged fish ranged widely through the Coral and Tasman Seas, with tag deployment times reaching 68 days and with displacements up to 1268 km between tag release and recovery.

A robust model was developed for estimating not only location, but also uncertainty from light-based positions. Historically this had been a substantial issue, as statistically independent estimates of uncertainty for light-based locations had not been readily available. This location model was incorporated into a statistical model of Swordfish behaviour, allowing the integration of all position data obtained from the tags including release and recovery locations, GPS estimated locations, and light-based locations. The resulting model was used to explore movement rates, seasonality in movement, location preferences, and site fidelity. Estimates were made for the parameters in each of these models, which are readily transferrable to other analyses.

Based on the outcomes of the analysis Swordfish do have site fidelity. There is also evidence that they do migrate to some extent, at least regionally in the Coral and Tasman Seas. The ultimate outcome of the analysis is that the fish would likely move outside any modest spatial management zone, although mixing at a larger scale is likely limited by site fidelity of individual fish. However, reducing fishing pressure in locations preferred by Swordfish would be expected to reduce fishing mortality to some extent, as the fish do appear to have appreciable site fidelity at a spatial scale of a few hundred kilometers. The movement estimates from the analysis are in a form that could be readily incorporated into other analyses, including spatially structured stock analysis models.

The project was able to achieve all of its objectives, with the exception of incorporation of data sets collected by other researchers. These data sets were not available in time to be included in the analysis, and thus did not form part of the results

KEYWORDS: Geolocation, State space model, Light, GPS, Tag, Hidden Markov model, Movement, Swordfish, Site fidelity, Stock structure, Migration.

2. ACKNOWLEDGEMENTS

The author would like to acknowledge the support of Ian Sutherland and the crew of *Annandale* and Pavo Walker and the crew of *Assassin*. Gary Heilmann and Mike Madden of Mooloolaba Fisheries Investments Pty Ltd provided considerable logistical support in organising tagging operations. Karen Evans (CSIRO), Matthew Horsham (CSIRO), David Kube (CSIRO) and Matt Lansdell (CSIRO) are thanked for their assistance on the project both in the laboratory and at sea. Marinelle Basson (CSIRO), Mark Bravington (CSIRO) and Jason Hartog (CSIRO) provided substantial assistance in the development of various computational and statistical aspects of the project. Tagging operations were carried out under DPIW AEC permit 08/2007-08 and under scientific permits 1001144 and 1001375 issued by the Australian Fisheries Management Authority.

3. BACKGROUND

Swordfish have been one of the primary species driving the development of the domestic pelagic longline fishery off the east coast of Australia since its rapid expansion in 1997. The intense targeting of Swordfish has resulted in localized depletion of stocks off the east coast, particularly in the region off southern Queensland (Campbell and Hobday 2003). As catch rates in the nearshore regions declined, vessels moved offshore, resulting in an expansion in the fishery and growth in the zone of localized depletion (Campbell and Hobday 2003). The need for management measures to address this localized depletion was recognized in several Eastern Tuna and Billfish Fishery Resource Assessment Group (ETBF RAG) meetings over the in the mid 2000's, and the group discussed measures to rectify the situation including spatial restrictions or closures and gear restrictions.

Based on CPUE patterns and fish size monitoring at processing plants, the stock harvested off the east coast is thought to be largely a regional stock, spawning in the Coral Sea, and then migrating to foraging grounds to the south in the Tasman Sea and to the east off the east coast of the North Island of New Zealand. This assumption is supported by genetic studies, which suggest that the Pacific Swordfish stocks follow a backwards "C" shaped pattern, with the strongest isolation between Japanese and Australian stocks, both of which are somewhat related to stocks off the west coast of the Americas (Reeb et al. 2000).

However, the establishment of spatial management measures requires detailed information on movement patterns beyond these rough regional patterns – information which was largely unavailable, with conventional tagging programs limited by low deployment and recovery rates, and no electronic tagging studies completed at the time. In the context of this immediate need for information to support management CSIRO initiated an electronic tagging study to understand Swordfish movements into and out of the region of localized depletion, focusing on the data essential for developing an effective management response.

As the need for measures to address the local depletion off the east coast was developing, CSIRO and the National Institute for Water and Atmospheric Research of New Zealand were finishing a draft stock assessment for Southwestern Pacific Swordfish (Kolody et al. 2008). This assessment identified regional movement patterns and connections with the central South Pacific stocks as fundamental uncertainties in our understanding of regional Swordfish dynamics.

This project was developed in the context of these two ongoing efforts, with the goal of investigating the linkages with the central South Pacific stocks by extending tagging efforts to the Coral Sea spawning grounds, a likely site of interchange between domestically harvested stocks and those outside the Coral/Tasman region. The minister for fisheries issued a directive instructing AFMA to develop harvest strategies for Commonwealth fisheries considering the impacts of not only domestic effort, but also effort by other nations' vessels which harvest shared stocks. This directive brought the need to identify the boundaries of stocks harvested within the AFZ and the amount of mixing with stocks outside the AFZ into sharp focus, both to allow AFMA to set domestic policy and to support advocacy of the Australian position internationally in RFMOs. Additionally, the directive instructed AFMA to investigate spatial management for commonwealth managed fisheries, which necessitated a clear understanding of movement, migration, and residence patterns for both target and non-target species caught during fishing operations.

4. NEED

Knowledge of the stock structure and migration patterns is fundamental to ensuring effective stock assessment and management of a fishery. While this knowledge is scanty for many Commonwealth fisheries, Swordfish structure and movements were particularly poorly known at the time this project was developed. The stock harvested by the ETBF was locally depleted at the time this project was developed, suggesting population structure, but there were no direct data on movement or distribution available. Parameterizing a model of movement for Swordfish would clarify the stock structure and provide a mechanism for incorporating their movements into spatial management or assessment models.

The Ministerial Directive to AFMA issued just prior to the funding of this project highlighted the lack of knowledge regarding Swordfish. Key initiatives in the directive were 1) develop harvest strategies for its fisheries to ensure sustainable management; 2) recover overfished stocks; and 3) end overfishing on stocks. Furthermore, the directive urged AFMA to move to spatial management. Critical to the design of harvest strategies, determination of stock status, and development of spatial management measures is a sound knowledge of the connectivity between stocks fished locally and in other parts of the Pacific basin. In order to ensure equity in limitations due to management arrangements, Australia also needed to pursue policies that ensure other nations protect shared stocks within the context of the Western Central Pacific Fisheries Commission - requiring clear evidence of the amount of movement between locally and regionally harvested stocks and empirically validated assessment models.

The March 2005 AFMA/ComFRAB Research Gap Analysis and Priority Setting Workshop, held jointly by AFMA and ComFRAB underlined the needs outlined above for Swordfish in the ETBF specifically – identifying both spatial management measures to rectify the localized depletion and provision of science and policy advice into the WCPFC. The ETBF research priorities and FRDC's strategic challenges both identified these same issues, as discussed in the Background section.

5. OBJECTIVES

This project had the following five objectives:

1. Collect Swordfish movement data and habitat preferences on the Coral Sea spawning grounds and during subsequent migration using electronic tags;

2. Collate data from this study with data from ongoing studies on Swordfish movement in the Tasman Sea, east of New Zealand, and in the central South Pacific spawning area;

3. Refine existing analysis methods to incorporate electronic tag data and oscillatory movements such as annual migrations;

4. Parameterize a regional movement model which describes retention times on the spawning grounds and migration patterns; and

5. Provide a succinct description of stock structure and movement that can be incorporated into other analyses.

In order to achieve these objectives this project encompasses three major components: 1) the deployment and recovery of tags; 2) development of novel methods for analysing light-based geolocation data and individual scale path-based movement behaviour; and 3) analysis of retention times, aggregation patterns, and migration dynamics of Swordfish off the east coast of Australia and throughout the broader south-western Pacific Ocean.

6. METHODS

6.1 SATELLITE TAGGING

Tagging operations for this project followed those developed by the author and collaborators in a similar project focused on the deployment of electronic tags on Swordfish throughout the Tasman Sea (AFMA Project 2006/809). Operations are primarily focused on the period October to March and from vessels operating out of Mooloolaba, Queensland. In an effort to maximize the success of deployments and minimize any adverse effects on tagged animals, criteria developed by the authors from previous deployments of electronic tags on Swordfish were used in identifying potential candidates for tagging.

Under these criteria each candidate fish must:

1. be alive;

2. be greater than 150cm from the eye to the fork of the tail (orbital fork length or OFL, translating into a weight of at least 50-60kg);

3. be highly vigorous;

4. have a swim bladder that is not inflated (i.e. the fish is not floating at the surface);

5. be hooked in the mouth only;

6. not be bleeding profusely.

The use of these criteria lead to an average of one Swordfish suitable for tagging for every two longline sets, given the vessel was targeting Swordfish. However, by following these criteria the deployment life of the tags was increased, with nearly half of the tags reaching their planned deployment period (Table 2, Figure 1). Procedures followed in the tagging of each fish were carried out under protocols developed by the Pelagic Fisheries and Ecosystem Stream within CSIRO Marine and Atmospheric Research and approved by the Australian Ethics Committee through the Department of Primary Industries and Water, Tasmania.

Tagging operations were conducted from FV Annandale and FV Assassin, and in general trips have encompassed the area between 154°E and 160°E and 24°S and 29.5°S. Tagging was based on a scientific technician accompanying the vessel on commercial trips. During longline hauling, fish suitable for tagging were identified, a weight was agreed between the vessel captain and the technician, the fish was tagged in the water using a pole to insert an anchor with a tethered tag into the pterygiophores (the bones anchoring the dorsal fin) and the fish was subsequently cut loose. Estimated weights were the weight gilled and gutted. The vessel was subsequently compensated according to an agreed price based on the estimated weight.

Estimated weights were converted into length using allometric relationships estimated by Dr. Robert Campbell based on fisheries observed data from the Eastern Tuna and Billfish Fishery (pers. comm). The allometric relationship is:

Headed&Gutted-Weight (kg) = a.Length(cm)^{b}.

The parameter estimates for these relationships are shown in the Table 1.

Table 1. Allometric relationship parameters estimated from Swordfish taken in the Eastern Tuna and Billfish fishery.

	A	B	R^2	SAMPLE SIZE
HGW = A.LENGTH^{B}	3.939X10^{-5}	3.2516	97.51 %	2000

WW: whole weight, HGW: headed and gutted weight. Length is in cm, weight in kg.

Tag deployments were much slower than initially expected for a number of reasons. There was a major shift in fishing activity from 2007 onward, with a large reduction in targeting of Swordfish from commercial vessels. This was related to at least two factors. First, there was a sharp increase in the cost of fuel. This reduced the viability of fishing for Swordfish, as trips were frequently very far from shore due to reductions in historic catch rates nearer shore. Second, during the project a number of operators who had traditionally pursued Swordfish and other species using shallow sets adopted an additional mode of fishing with deep-set hooks. This change in fishing strategy increased Albacore Tuna and Bigeye Tuna catch, but decreased Swordfish catch rates substantially. The new methodology appears to have been driven to some extent by an increase in the price for Albacore, potentially due to new market opportunities.

As proposed in the June 2010 milestone report the number of tags deployed was reduced from the original 15 to 14. While the milestone suggested that only 13 might be possible, there was an opportunity to deploy one additional tag leading to a total of 14. The tags used in the project were PSAT Mk 10 tags from Wildlife Computers Inc. They were a newly developed tag that incorporated both light and GPS for estimating location. Light data is notoriously difficult to analyze for species that dive on dawn and dusk, as do Swordfish. The opportunity arose to trial these newly developed towed tags, which could also record GPS data if the fish was at the surface. Preliminary trials indicated that Swordfish basking behavior provided adequate opportunity for collection of GPS data, and thus a decision was made to change to the mixed light and GPS tags.

6.2 DATA ANALYSIS

6.2.1 Tagging data

A total of 14 electronic tags were released on live Swordfish meeting the criteria outlined in the methods. Fish ranged in size from an estimated maximum dressed weight of 240 kg to an estimated minimum dressed weight of 55 kg. Visual estimates of weight are likely to be relatively inaccurate, and on two occasions there were inconsistent estimates between the scientific

technician and the vessel captain. Adjusting the weights using the technician's estimates of length following allometric relationships from the Methods section, the maximum weight was 150 kg. The mean weight for the tagged fish after adjustment was 82.6 kg, with a standard deviation of 27.6 kg.

Table 2. Information on timing and size of Swordfish tagged.

SMART ID	RELEASE DATE	RECOVERY DATE	FULL DURATION	TIME AT LIBERTY	ESTIMATED LENGTH (CM)
36861	28/02/08	5/03/08	NO	6	169.7
37702	23/03/08	23/04/08	NO	31	160.0
39796	6/11/08	4/01/09	YES	59	161.8
39969	25/03/08	23/05/08	YES	59	190.0
39970	12/12/08	9/02/09	YES	59	NA
83860	8/11/08	21/11/08	NO	13	157.5
83861	13/12/08	10/02/09	YES	59	NA
83862	19/06/08	17/08/08	YES	59	189.3
83863	15/12/08	12/02/09	YES	59	NA
83864	25/05/08	2/06/08	NO	8	169.7
84184	10/12/09	6/02/10	NO	58	214.5
84186	7/12/09	23/01/10	NO	47	183.3
86588	11/12/09	17/02/10	NO	68	169.7
86589	6/12/09	8/12/09	NO	2	180.1

Based on past studies, animals with orbial fork lengths (OFLs) greater than 220 cm are female, those with measurements 180 cm or greater are more likely to be females, animals shorter than 180 are mixed sexes (Young and Drake 2002). Using these break points between categories, one tag (84184) was attached to a female fish, while 4 others are very likely to be on females. Attachment periods ranged from 2 to 68 days. Attachments were set for between 2 and 9 months. While 4 tags detached prematurely in a very short period, the remaining 10 tags gave a significant temporal coverage.

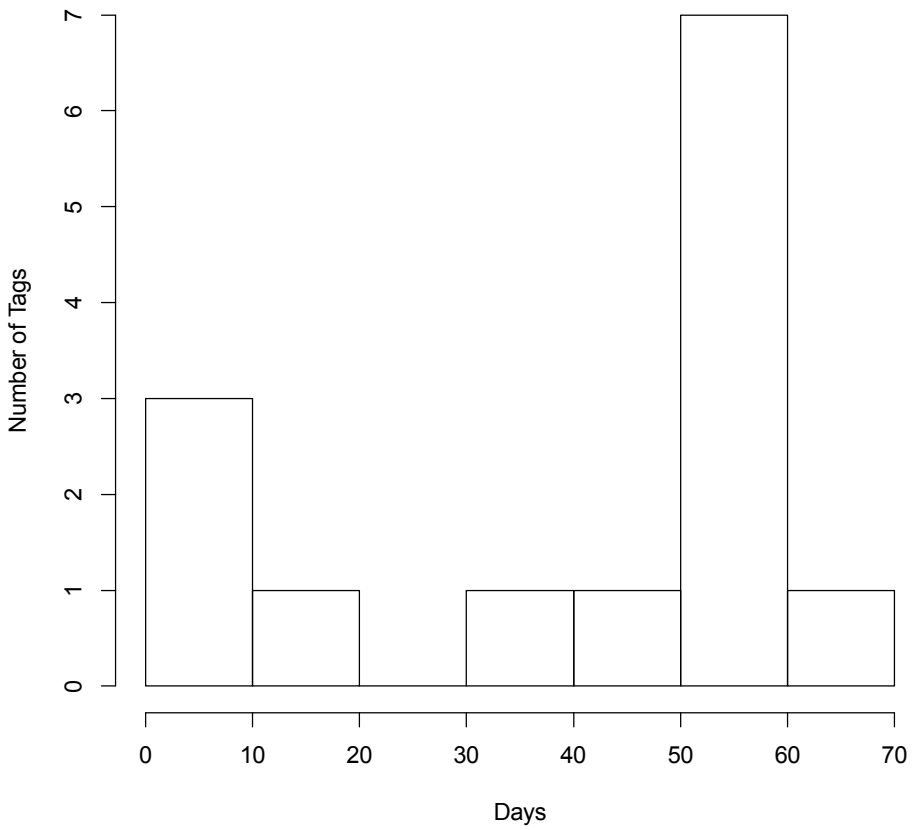

Figure 1. Deployment lengths of electronic tags.

Across the 14 tags released in the study, data was collected on 277 occasions which could be used in estimating positions, including release locations, GPS satellite transmissions, light readings, and recovery locations. Of these data sets, 187 were sets of light readings, 62 were sets of GPS satellite transmissions. The 14 release locations were known from the tagging vessel GPS and the corresponding 14 recovery positions were given by the Argos system as a byproduct of data transmission.

There were issues with a large number of the light positions, due to the diving behavior of Swordfish and other unknown factors. Swordfish frequently dive on dawn and surface at dusk, neutralizing the available light signal. In addition, it is possible that the software on the tags may interact with Swordfish behavior to complicate the recording of accurate light positions. Multiple light positions were often recorded within relatively short periods of time, which would suggest something is triggering the tag to record a false dawn or dusk event. Due to these complications the software from the tag manufacturer was able to produce only 2 useable light positions from the 187 sets of light readings taken during the tag deployments. This issue points to a critical

need for an estimation algorithm that can accommodate the complexities in this data, rather than losing the vast majority of it. This is the focus of the analysis presented in section 6.2.3 below.

6.2.2 Analysis of raw position data

We analysed the raw position data provided by the tag manufacturer's software using a combination of graphic techniques and generalized linear models. Notably, this analysis does not include any consideration of uncertainty in the positions, so it is largely limited to positions which are expected to have small uncertainty, such as tag deployment and release positions.

The focus of the analysis was on evaluation of evidence for local residency. The methods are drawn from Turchin (1998), who describes an approach for evaluating the relative evidence for linear movement, diffusive movement, and philopatric (having site fidelity) movement based on comparison of the relationship between displacements at two successive periods. Linear movement is expected to result in displacements that scale linearly with the time between positions, diffusive movement should result in displacement scaling with the square root of time, and philopatric movements should show an asymptotic relationship with time. We utilize linear regression to explore the relative support for these three functional relationships, and evaluate the resulting support using AIC (Burnham and Anderson 2002).

It is important to note that this should be considered an exploratory analysis, as it uses a relatively small portion of the data available. However, it has the benefit of being completely independent of the more complex state space model described in 6.2.3 and 6.2.4.

6.2.3 Developing a likelihood for location based on light data

Conceptual framework for the likelihood of light observations

A standard approach for estimating parameters, θ, for a relationship of interest given data, D, is to use their likelihood function, $\Pr\{D|\theta\}$, to calculate the probability of a set of observations, or data, given particular values of the parameters. Maximizing this probability, one can then find the maximum likelihood estimates of the parameters, $\hat{\theta}$, given the data. In addition, one can calculate the relative probability of other values of the parameters, which allows the construction of confidence intervals around the maximum likelihood estimates. However, this approach requires a detailed probability model that gives the probability of a set of data given particular values of the parameters.

In the case of light-based geolocation, it is not possible to specify this detailed probability model. Therefore, we utilize an alternative approach which takes advantage of our ability to know the true value of the parameters of interest in a special case, i.e. the location of a mooring position at which light data is taken. Combining this information with Wilke's theorem we can calculate an approximate relative likelihood for light data given a location.

As a first approximation we can estimate the parameters, i.e. the latitude and longitude, that determine the observed light data using the difference between the observed and the expected light values. A simple measure of this difference is the sum of squared deviations between these

values. By minimizing these values we can find the best fitting parameters, i.e. latitude and longitude, for a given light curve. However, as we cannot assume that these differences are Gaussian distributed and uncorrelated, therefore the sum of squares is not a proper likelihood, but only a measure of fit.

For the geolocation application we refer to the parameter vector of latitude and longitude as θ, with $\hat{\theta}$ denoting estimated values, θ_{true} the known values at the mooring, and $\hat{\theta}_{\min}$ the values that minimize the difference between observed and expected light readings. The quantity we would like to know, is given $\hat{\theta}_{\min}$ for a particular light curve, how much less likely is any other location θ.

Given that we know the true value of the parameters, i.e. the latitude and longitude of the mooring location, we can calculate the difference between the observed and expected values at the true location, θ_{true} for a set of light data from a twilight event. We can also find the difference between observed and expected light values at $\hat{\theta}_{\min}$ for the same set of light data. From these two sums of squares, we can calculate the difference in sums of squares between θ_{true} and $\hat{\theta}_{\min}$, or δ_{SSQ}. Using a set of observations of the values of δ_{SSQ} across *N* twilight events it is then possible to construct an empirical probability distribution as

$$F(\delta_{SSQ}) = \frac{1}{N}\sum_{i=1}^{N} I\left[SSQ(\theta_{i,\min}) - SSQ(\theta_{i,true}) < \delta_{SSQ} \right], \quad (1)$$

Where *I* is an indicator function that has a value of 1 if the condition is true for the i^{th} observation, and 0 otherwise. This distribution gives the probability of observing a difference in sums of squares of a given size or smaller between the true location and the best-fit location for a given light curve.

However, the goal is to be able to express the relative difference in likelihoods at two possible locations, not the difference in sums of squares. Thus we need a method to scale the difference in sums of squares to a difference in likelihoods. To do this, we turn to Wilke's theorem, which relates the ratio of two likelihoods to a known distribution. Wilke's theorem states that as sample size, *n*, approaches infinity the log of the ratio of two nested likelihood functions, *x*, will be distributed as one half times chi-square distribution with degrees of freedom, *d*, equivalent to the dimensionality of the parameters of the likelihoods

$$\Pr\left\{ \ln\left(\frac{L\{\theta' | D\}}{L\{\theta'' | D\}} \right) = x \right\} \propto \frac{1}{2}\chi_d^2(x). \quad (2)$$

Defining the inverse of a probability distribution as the function, *G()*, which returns the value at which the cumulative density function, *F(x)* takes on a particular probability, that is

$$G(F(x)) = x, \quad (4)$$

we can rearrange Wilke's theorem to relate one likelihood to another,

$$L\{\theta' \mid D\} \propto \frac{1}{2} G\left(\int_0^x \chi_d^2 \, dx \right) L\{\theta'' \mid D\}, \tag{5}$$

where

$\left(\int_0^x \chi_d^2 \, dx \right)$ is the cumulative density function of the χ_d^2 distribution evaluated at *x*. Thus, from Wilke's theorem, if we know how probable a difference in log likelihoods is, i.e. the value of the cumulative density function of $\frac{1}{2}\chi_d^2$, we then know the ratio of the likelihoods from the inverse of the χ_d^2 distribution. Although we do not know the actual likelihoods in (5), we do know how likely a given difference between them is as we constructed an empirical cumulative density function for the difference in (1), although it was measured in sums of squares. Substituting from (1) we get

$$L\{\theta' \mid D\} \propto \frac{1}{2} G\left(F\left(\delta_{SSQ}\right)\right) L\{\theta'' \mid D\}, \tag{6}$$

where G() is still the inverse function of the χ_d^2 distribution, but the cdf of the χ_d^2 distribution has been replaced by (1), the empirical cdf of the difference between the two likelihoods measured by their sums of squares.

Thus Wilke's theorem provides a means to estimate the difference in likelihoods between the best estimate for the location of a twilight event, $\hat{\theta}_{\min}$, and any other location θ. Given the δ_{SSQ}, we calculate the cumulative density function for a difference this large $F\left(\delta_{SSQ}\right)$. We use this probability in the inverse of the χ_2^2 distribution to get the ratio between the likelihood at $\hat{\theta}_{\min}$ and the other location θ. The χ_d^2 distribution has a dimension of two, as we are estimating a longitude and a latitude. It is important to keep in mind that this is a relative likelihood, as we do not know $L\left\{\theta_{\min} \middle| D\right\}$. However, a relative likelihood is sufficient for modelling movement in this case, as we are only concerned with comparing the relative likelihood of the set of possible locations given light data, not in determining the absolute likelihood of a given location.

Estimating the likelihood from mooring data

The first step in estimating the likelihood function is to develop a relationship between the light intensity measured on the tag's sensor and the location and time at which that measurement was taken. These two quantities are linked by the angle of the sun. The intensity of light measured should have the same expected value at any point on the earth for a given sun angle, and the sun angle can be predicted if the location and time are known. Thus, given a known location and time we can estimate the response of the tag sensor to sun angle empirically from a set of its measurements of light.

We used data from a Wildlife Computers MK9 archival tag, moored off the west coast of the Australian continent at -33.93337 degrees latitude, 121.8501 degrees longitude from 23

November, 2008 to 23 February, 2009. The archival data from the tag, which consists of continuous light readings, was provided to Wildlife Computers, who kindly processed this data using analogous software to that present on their MK10 PSAT tags. These tags internally identify twilight events, then select a section of the archival record around the event, take evenly spaced samples of the light data during this period, and adjust this time series for the effect of depth on light intensity. The tags then store these data for later transmission. Wildlife Computers staff processed the data from the archival tag using this algorithm and returned the resulting compressed PSAT style data.

We used the established astronomical algorithms to calculate the altitude, or horizontal angle relative to the horizon, of the sun at the mooring location on the times when the light readings were taken by the tag (Meenus 1998). The light data was standardized by subtracting off the mean value of the light intensity during each twilight event. We used a Generalized Additive Model to estimate the relationship between the sun angle during twilight events and the standardized light intensity recorded by the tag, implemented in the MGCV package in the R statistical language (R Development Core Team 2010). This model was appropriate as the shape of the relationship is not known, and thus it was not possible to fit a parametric curve.

Once an estimated relationship between light intensity and sun angle was available, it was possible to evaluate the relative fit between an observed light curve and the predicted light at any given location. Using this relationship one can find the most probable location for an observed twilight event by minimizing a measure of the difference between the observed and predicted light readings. We use the sum of the squared deviations, SSQ, as discussed above, to measure this difference or lack of fit. Optimization problems were solved using the Optim package in the R statistical language (R Development Core Team 2010).

As a first step in validating this approach we estimated the best location, in terms of the sum of squared deviations between the predicted and observed light, for the light data taken during each observed twilight event at the mooring. As a minimum one would expect the model, if it were an accurate representation of the process, to identify positions at or near the mooring, and for those locations to be evenly distributed around the mooring. While this is not a completely independent test of the model, it provides some evaluation of whether the model can accurately predict location, given light data collected at a known time.

The deviations between the model predictions for light and the observations give a measure of the fit of the model to a given set of data. The next step in the analysis is to use the differences in the qualities of the fits at the known location and the fits at the best location to develop a likelihood surface for light observations given a position. We do this by calculating the sum of squared deviations at the location that minimizes the sum of squares $SSQ_{\min}$, and subtracting them from the sum of squared deviations at the known location SSQ_{true}, as explained in the previous section. Ordering these values from minimum to maximum, we then form the cumulative density function for the value of δ_{SSQ} from this empirical distribution of values as in (1) above.

6.2.4 Analysis of movement behaviour

There is significant diversity in the approaches that have been taken to analysing data from satellite tagging studies of marine species. The data are in essence time series data on the location and behaviour of the animal. However, they are complicated by the fact that positions are often uncertain and are not observed continuously. For Swordfish in particular these two complications are significant. The diving behaviour of Swordfish, descending at dawn and ascending at dusk, remove much of the signal in the change in light levels over the course of a day. This behaviour has two implications. First, it reduces the quality of light observations that could be used for geolocation. Second, due to this reduced quality, not only are positions often uncertain, but also there are often significant gaps of time between observations of a dawn or a dusk event that can even be used for light based geolocation. Similarly, for positions that are derived from satellites, either via Doppler shifts or from global positioning satellites (GPS), Swordfish only spend adequate time at the surface sporadically, resulting in position estimates that often have significant temporal gaps.

In this context any statistical approach to analysing Swordfish data must not only be able to include the various types of data related to location, including known positions of release and recovery, along with GPS and light data during deployment, but it must also be able to incorporate the uncertainty in the locations and accommodate significant temporal gaps between observations. State space models provide a useful tool for incorporating dissimilar data types and addressing the uncertainty in positioning from each of the types (Patterson et al. 2008). These models treat the location of the animal as an unobserved state. Observations, in this case of light levels or satellite distances, then occur with some probability, which is conditional on the unobserved location state. The model represents the change in the unobserved state over time, with each successive state dependent upon the previous state. Observations are generally conditional only on the current state at the time the observation is collected. This process can be illustrated by a directed graph, which shows the relationships between the components in a state space model (Figure 2).

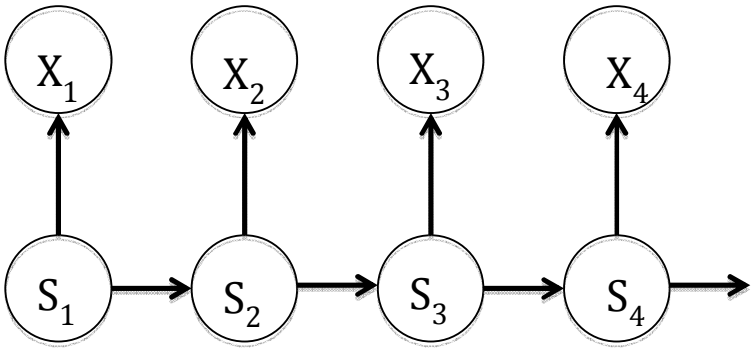

Figure 2. Directed graph of a state space model. The arrows indicate dependence in the graph, while circles indicate nodes. Here S_t is the (unobserved) state of the process at a given time, while X_t is the observation of the process at that time.

In reality animal movements happen continuously in time and space. However, mathematically it is sometimes more convenient to divide either space or time, or potentially both, into discrete

units. In the case of the Swordfish we chose to represent this process discretely in both space and time as hidden Markov process (Zucchini and MacDonald 2009), in which

$$\Pr\{X(t)|\mathbf{S}(t-1),\mathbf{X}(t-1)\}=\Pr\{X(t)|S(t)\},t\in N \quad (7)$$

and

$$\Pr\{S(t)|\mathbf{S}(t-1),\mathbf{S}(t-2),...\mathbf{S}(1)\}=\Pr\{S(t)|S(t-1)\},t=2,3,..., \quad (8)$$

where *X(t)* and *S(t)* are the observation and the state respectively at time *t*. Note that the vector ***X(t)*** of all observations up to time *t* is only dependent upon the state at time *t* (Figure 2). The Markov property also implies that the state is only dependent upon the state at the previous time. These two assumptions simplify the problem substantially.

In order to implement this we represent the state dynamics as a transition matrix, Γ, which describes the probability of moving from any location i to another location j in one unit of time, p_{ij}, and a state vector, *s(t-1)* which represents the location of the animal at the preceding time step, *t-1*, thus

$$\Pr\{s(t)|s(t-1)\}=\Gamma s(t-1) \quad (9)$$

where

$$\begin{matrix} p_{11} & . & . & p_{1M} \\ . & p_{21} & & \\ . & & . & \\ p_{M1} & & & p_{MM} \end{matrix}, \quad (10)$$

and

$$s(t-1)=\begin{bmatrix} q_1 \\ . \\ q_M \end{bmatrix}. \quad (11)$$

In this context the state at any time is represented as a vector of probabilities, q_i, that the animal is in each of the *M* possible locations.

The model can be extended to include variation in the state transitions as a function of individual or environmental features by incorporating covariates, *Y*, and a set of corresponding coefficients, β, into the state transition probabilities. However, to ensure that these values are probabilities, i.e. are bounded by the interval (0,1), we introduce an intermediate value o_{ij}

$$\text{logit}\left(o_{ij}\right)=\beta Y, \tag{12}$$

which we then normalize to calculate the transition probability between locations i and j as

$$p_{ij}=\frac{o_{ij}}{\sum_{j=1}^{M} o_{ij}}.$$

This normalization is equivalent irrespective of the equation that parameterizes the transition probabilities (12), and thus is not represented further. For clarity, we refer to the parameterization of the transition probabilities by their intermediate value, o_{ij}.

In the model developed for the Swordfish we decomposed this quantity into two components, one that expresses the attractiveness of a location an animal might move to and a second, which incorporates the distance from the current position. The function is of the form

$$\text{logit}\left(o_{ij}\right)=\beta Y+e^{-\alpha D_{ij}}. \tag{13}$$

Here D_{ij} is the distance between location *i* and *j*, and α is a parameter scaling the effect of this distance. It is essential to incorporate distance in this context in any model evaluated, as there is an expectation that animals will be less likely to move to a given location as the distance between it and their current location increases.

In order to accommodate the temporally sparse nature of the observations for Swordfish, it is necessary to project the unobserved state over the time between observations. Here we assume that the relevant covariates for determining the state dynamics are limited to those at the time of the next observation, $t+\Delta t$, ignoring the effects of covariates between the current time and the time of the next observation time. This means that the probability of transition becomes

$$\Pr\left\{ s\left(t+\Delta t\right)|\, s\left(t\right)\right\}=s\left(t\right)\prod_{t}^{t+\Delta t}\Gamma \tag{14}$$

with

$$\text{logit}\left(o_{ij}\right)=\beta Y_{t+\Delta t}+e^{-\alpha D_{ij}}. \tag{15}$$

In order to implement this model, we also need to specify the probability of the observation given the state, $\Pr\left\{ X(t)\right\}$ as in (7). Recalling that the probability of an observation *x* is only dependent on the state, we can write

$$\Pr\left\{ X(t)\right\}=\mathbf{P}_{s,t}\left(x\right)\mathbf{S}\left(t\right). \tag{16}$$

The probability of a particular observation $\mathbf{P}_{s,t}\left(x\right)$ depends on the state *s*, which in this case is the location of the animal, and the known time *t* at which the observation(s) are taken. This probability is a vector, as there is a probability for the observation for each of the possible

locations. The unconditional probability of the observation must also account for the probability of being in each possible state, $\mathbf{S}(t)$. Expressing this probability as a vector product is equivalent to summing over all of the possible states.

We have four types of observations related to the locations of Swordfish, direct observations of locations at the release and recovery times, and light readings and GPS location estimates. We assume that the release and recovery observations are made without error. Thus in each of these cases $\mathbf{P}_{s,t}(x)$ is a vector with a one in the state corresponding to the release location, and zero in all the remaining entries. We also treat the GPS locations as observations without error. While this is not strictly accurate, the error in the GPS locations is small enough that relative to the spatial resolution of the state that it is very unlikely there is any uncertainty as to which state the animal is in if a GPS reading has been made. Observations of light are not unambiguously related to being in a single location, thus for light observations $\mathbf{P}_{s,t}(x)$ is a vector of probabilities each corresponding to the probability of the light recorded on the tag conditional on the animal being in the corresponding state at time *t*. We do not have an explicit model for these probabilities, thus we use (6) to calculate the relative likelihood relative of the light observation given the location.

We used the hidden Markov model developed above to answer three questions:

1. Is there spatial variation in habitat preference in the Coral and Tasman Sea region?

2. Is there evidence of a seasonal migration in Swordfish?

3. Do Swordfish show site fidelity?

These questions were each posed as a hypothesis by altering either the first or the second term on the right hand side of (15). In all cases the base model included a parameter for the second term in (15) as there is an expectation that animals are less likely to move to locations that are further from their current location.

We investigated seasonal movements by dividing the set of possible locations up into a set of bands or blocks, and asking whether movements to these locations varied between the spawning and non-spawning season. The region was divided into blocks at 3 different scales, 2 blocks, 4 blocks, and 8 blocks (Figure 3).

Figure 3. Spatial blocking arrangements used in the analysis of electronic tagging data.

The model included a main effect for block locations, and an interaction term for the spawning season effect. The spawning effect was coded as a simple binary variable, depending on whether the observation was taken during the spawning season or outside of it. The spawning period was November to March, with the non-spawning period in the remainder of the year (Young and Drake 2002). We compared these models with a reduced version that included only the spatial block effect.

We investigated the possibility of site fidelity by fitting a model that included a covariate for the distance from the tagging site. This model thus has two distance effects, one for the distance between subsequent moves, which is the base model, and the second for the distance from the tagging location. The underlying assumption is that if the animals have site fidelity, the most likely place to tag them is in the location where they show the fidelity. If there is site fidelity, subsequent movements should be biased back toward this location.

The analysis was implemented on a spatial grid with a one degree latitude by one degree longitude resolution that spanned from -45 degrees to -10 degrees latitude and 145 East to 170 East longitude, equating to 936 possible grid locations. Other resolutions and coverages would be possible; however, we found this one to provide coverage of the area of interest, adequate resolution given the uncertainty in the tagging data, and a reasonable computational load to be implemented on readily available desktop machines. All analyses were conducted assuming a single day as the time step, again a compromise between resolution and computational speed.

The hidden Markov models for Swordfish movement explained above were fitted in the R statistical language using purpose written code following the methods in Zucchini and MacDonald (2009). We used the maximum likelihood approach developed there, treating the tag data as a set of independent time series, one for each tagged fish. Maximization of the likelihood was done using the optim function in R, which implements a Nelder-Mead algorithm, although we explored the use of a quasi-Newton method (i.e. BFGS in the optim function), and a second optimization routine provided in the nlminb function in R. Confidence intervals were calculated based on the negative of the expected value of the Hessian matrix, estimated during fitting by optim. In cases where we were unable to calculate the standard errors via the Hessian, we explored them using the profile likelihood method (Zucchinni and MacDonald 2009).

7. RESULTS/DISCUSSION

7.1 TAGGING DATA

Tagging deployments were relatively successful. Early efforts to tag Swordfish from commercial longlines had been relatively unproductive due to a mixture of post release mortality and tag shedding. In previous work approximately 43% of tags either released within the first two weeks of deployment due to shedding, or did not report (Evans 2010). In this study we were able to reduce early losses and non-reports (combined) by tags to 29% of the tags deployed, a substantial improvement over previous studies. Moreover, most short deployments remained attached and functional until their programmed release date.

There were a total of 187 light-based positions, 62 GPS positions, 14 release positions, and 14 recovery positions across the tags that were deployed. The release, recovery and GPS positions are given in Appendix 3; however, only the two light positions that were estimated by the manufacturer's software are provided. Due to diving behaviour of the Swordfish and potentially tag sensors and software, many of the light curves collected by the tags appear to contain minimal information on position. In particular the light positions were affected by variation in the number of light readings reported, dawn or dusk events identified that were too close in time to be possible, and dawn and dusk events that either had no change in light, or had patterns that suggested that the light data was corrupted, such as increasing and subsequently decreasing light levels within a single dawn or dusk event.

7.2 INFERENCE FROM RAW POSITIONS

Across the 14 tags that were deployed, the maximum displacement between the release and the recovery locations was 1246 km over a deployment period of 59 days. This gives an average rate of displacement of 21.11 km per day. Across the 14 tagged fish, the median

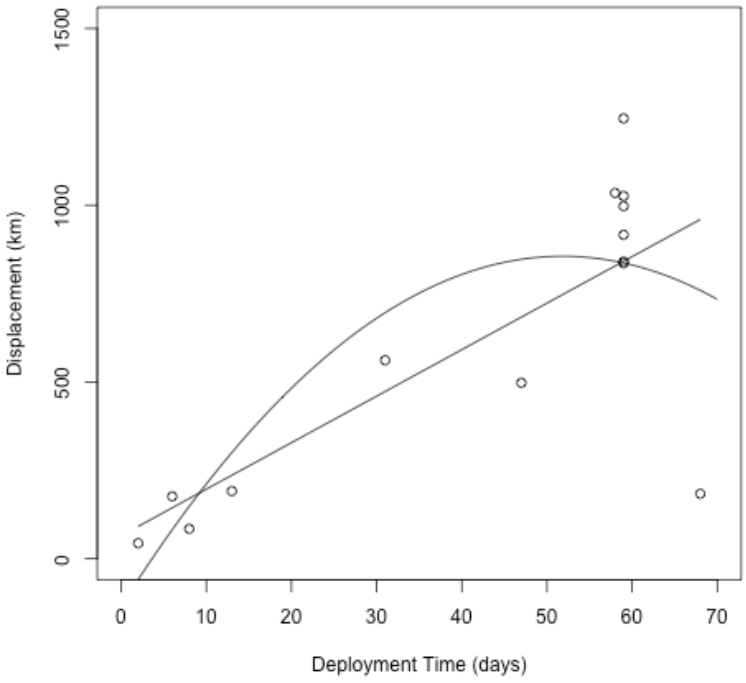

Figure 4. Distance between tag deployment location and tag recovery location. The lines show the first and second order linear regression fits to the data.

displacement was 836.1 km between the tag deployment and the recovery locations. The displacement ranged from a minimum of 43.9 km up to a maximum of 1246.0 km.

Displacement distances generally increased with the length of the deployment (Figure 4). Displacement was strongly related to deployment time, with a linear regression of displacement on deployment time explaining 56% of the variation in the data (Table 3). Based on the regression, the displacement distance increases by approximately 13 km per day.

Table 3. Regression statistics for the effect of deployment time on displacement between tag release and recovery locations for Swordfish.

	Coefficient	Standard Error	T value	Pr(>|t|)
Intercept	65.208	152.168	0.429	0.6759
Time Difference	13.158	3.167	4.154	0.0013 **
Adjusted R-squared: 0.5557, F-statistic: 17.26 on 1 and 12 DF, p-value: 0.001336				
Intercept	-133.631	200.363	-0.667	0.519
TimeDifference	38.186	17.576	2.173	0.053
$(\text{TimeDifference})^2$	-0.369	0.255	-1.446	0.176
Adjusted R-squared: 0.5927, F-statistic: 10.46 on 2 and 11 DF, p-value: 0.002854				

The regression relationship (Table 3) provides a means of predicting the spatial area occupied by a single fish with time, and thus could be used to infer mixing rates across larger distances. This linear relationship would suggest that the fish continue to spread as time passes, and thus stocks would be well mixed.

However, if fish have site fidelity one would expect the displacements to increase with time for shorter deployment periods, but then cease to increase once enough time had passed for the fish to cover the entire area it uses. Using the linear increase in distance would give erroneous predictions, as it would suggest that the fish would continue to spread at a constant rate. If there is site fidelity, including a second order term in the regression should improve the fit of the model, and it should have a positive first order term and a negative second order term. For the Swordfish tagged off the east coast of Australia, there does appear to be some weak evidence for site fidelity. A second order regression has a positive first term and a negative second term, and does fit the data slightly better (Table 3, Figure 4).

While the more complex second order model has an AIC value that is slightly lower (200.5 v 201.17), it only fits the data marginally better than the first order model. The AICs for nested models should differ by at least 2 for a more complex model to be considered significant improvement (Burnham and Anderson 2002). A likelihood ratio test for nested models gives a similar result, with a marginal improvement in the model which is not significant at the $p = 0.05$ level (Chi-squared 1 d.f. = 2.435, p value = 0.119).

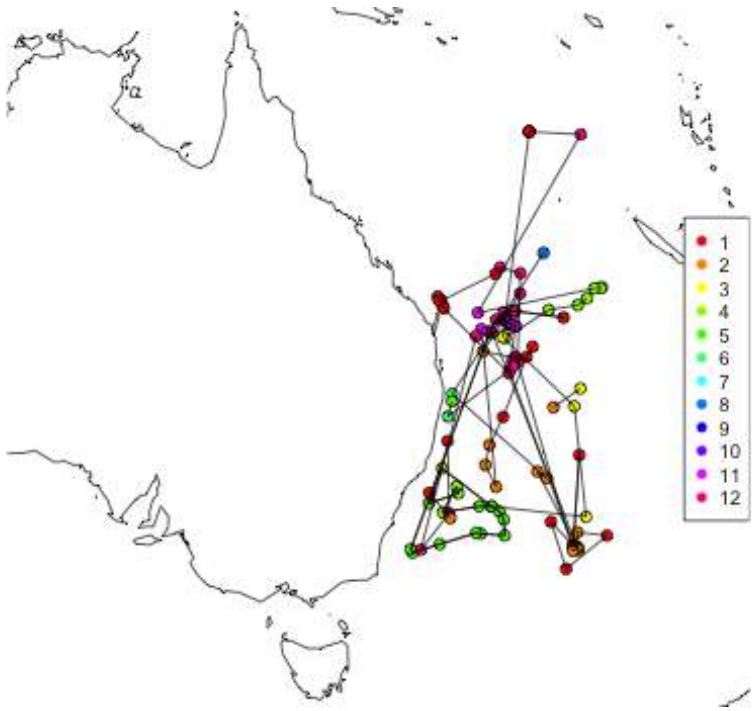

Figure 5. Locations returned from tagged Swordfish. The legend shows the month during which each location was recorded.

The possibility of site fidelity can be seen in the general pattern across the tag deployments (Figure 5). Most tracks recorded involve fish turning back inward toward the center of the region. By contrast there are no apparent tracks where fish were making directed movements out of the region when the tag released.

7.3 GEOLOCATION

Developing a likelihood for light observations given location consisted of three steps. First, we needed to estimate the relationship between sun angle and light recorded on a tag. Second, we needed to develop an algorithm that would find the location that minimized the difference between the predicted light from the angle/light relationship and the observed light from a tag. Third, we needed to use this algorithm to build a cumulative density function for the difference in fit between the observed light at the true location and the observed light at the best fitting location, which we could use with Wilkes theorem to calculate the likelihood of a location given a light observation.

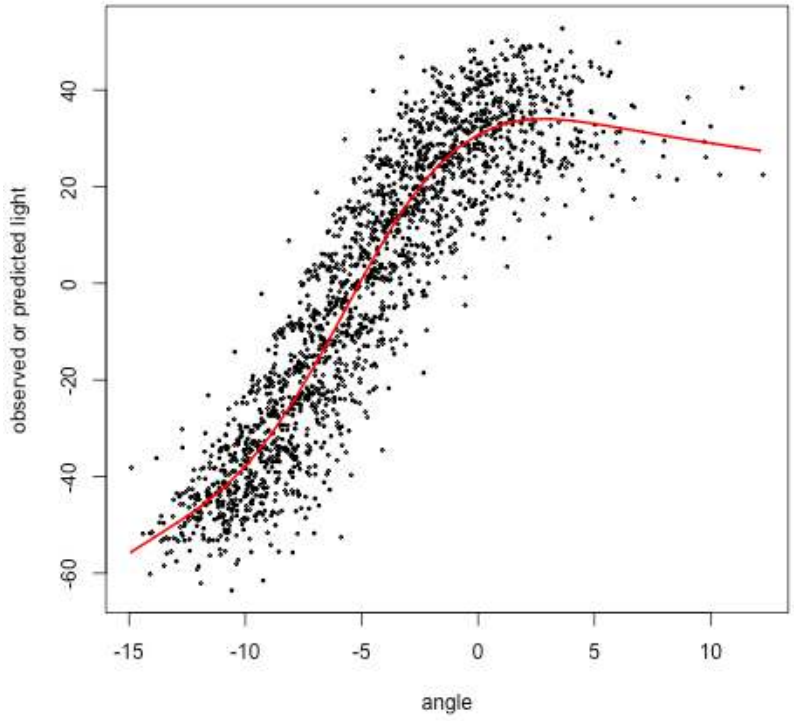

Figure 6. Responsiveness of the Wildlife Computers Mk 10 tag light sensor to sun angle. The red line is a generalized additive model fitted to the data using a smooth term for angle.

The data for estimating the relationship between the light intensity recorded on a tag and the sun angle and location was taken from a mooring located off Esperance, Western Australia (Figure 6). We used data from the moored tag starting on November 22, 2008 and running until February 22, 2009. The moored tag produced 183 light curves over this period, one for each twilight event (i.e. dawn and dusk). The light intensity data ranged from 31 units to 150 units.

The mean of the minimum light values across all curves was 45.5, with an average maximum of 131.8, and an average change of 86.3 over the course of a twilight event.

We explored a number of relationships to model this data, including a variety of polynomials, several nonlinear equations, and a smooth spline. Ultimately, the smooth spline gave the best fit and we did not pursue the other functional forms. The final spline model included an intercept term and a smooth term for sun angle with 6.24 effective degrees of freedom. The model explained 86.4% of the deviance in the data. Using this spline model we were then able to predict the light intensity that would be recorded on a tag given a particular sun angle.

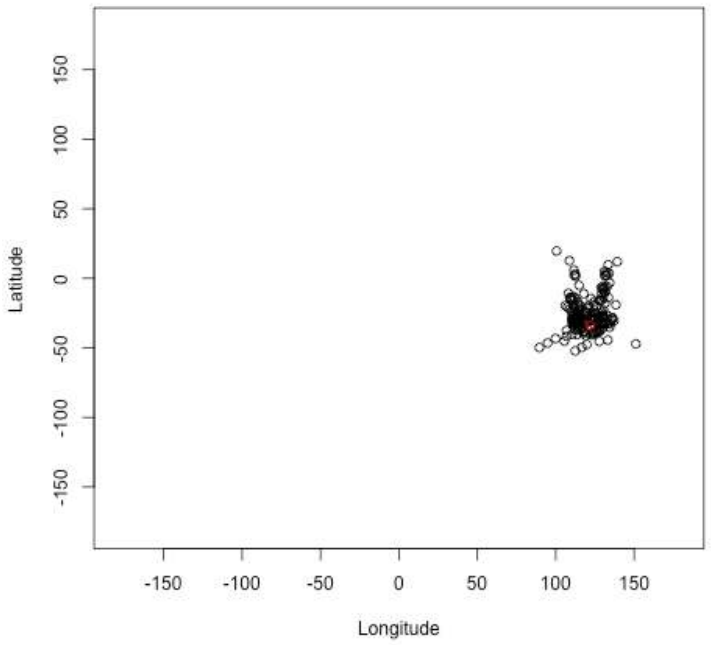

Figure 7. Best fitting locations for twilight events using light observed at the mooring off Esperance, Western Australia. The black circles show the estimated locations, while the red circle shows the actual location.

The second step in the development of the likelihood was to develop an algorithm for finding the location on the earth that most closely fits a light curve recorded at a given time. In order to do this we used the astronomical equations to predict the light angle at the time the observations were taken given a location. We then searched to find the location that gave predicted light intensities, based on the sun angle and the sun angle-intensity relationship (Figure 6), which most closely matched the observed light intensities. The difference between the predicted light and the observed light were measured using the sum of the squared deviations between the predicted densities and the observed densities.

Searches were done using the Optim function in the R statistical language to find the latitude and longitude that would minimize the sum of squares of the differences in light intensity (R Core Development Team 2010). We briefly evaluated the ability of the light intensity – sun angle model to allow us to determine the correct location of a light observation using the light intensity data from the mooring. The best locations of the 183 light curves from the mooring were centered on the mooring location (Figure 7).

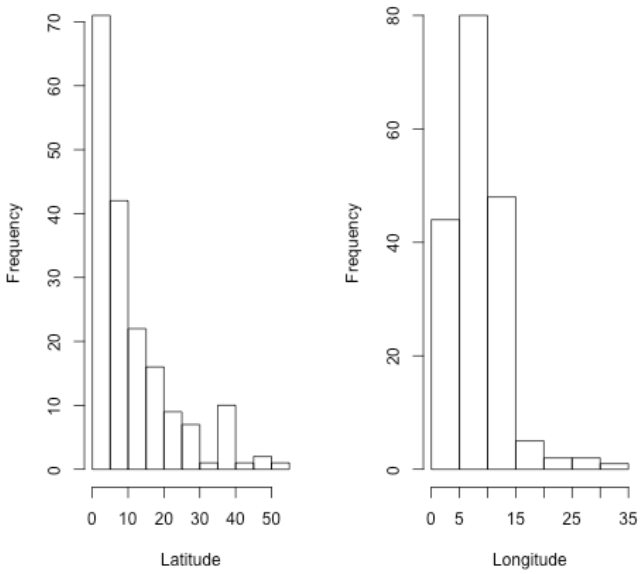

Figure 8. Distribution of displacement between the best fitting locations and the true location of the moored tag.

As can be seen from the histograms of distance however, geolocation using light still has significant uncertainty (Figure 8). Most latitude estimates are close to the actual location, but can be as far away as 60 degrees on occasion. Longitude estimates less variable, with all of the 183 estimates being within 35 degrees and most less than 15 degrees of the actual location. However, the most common longitude estimate is not in the region closest to the actual location, but slightly distant from it.

These variations are likely due to two sources. Light received by the tag is obviously affected by cloud cover. It may also be affected by other sources such as wave action, moon rises or sets that coincide with sun rises or sets, and possibly other factors. These variations in light could affect the tag in two ways. First, they might impact how the algorithm on the tag identifies a twilight event and selects the data to report later when the archival records are transmitted. Second, the variation in light intensity will also affect the measurements taken on the tag, even if the tag functions correctly and there is no variation introduced by the tag's on-board analysis.

It would potentially be possible to disentangle these sources of error as the mooring data was collected in full and processed into the compressed form returned by an archival tag subsequently by Wildlife Computers. For instance, records of cloud cover in the Esperance region could be correlated with variation in light readings, possibly allowing correction of those readings. However, for the ultimate application to archival tags that are being released from animals and transmit their data via satellite, these corrections would be useless. Light readings from tags deployed on fish will have unknown locations, thus applying a cloud correction to the data would be very difficult if not impossible. Therefore, while there is significant uncertainty in the

locations as illustrated by the best fit locations for the mooring data, it is important to include this uncertainty into the likelihood function for location given light data.

The best fit locations were utilized to estimate an empirical distribution of the difference in sums of squares between the light reading at the true location and that at the location that minimized the difference between the observed light and the light readings predicted for that location. The resulting distribution of ΔSSQ values rises fairly sharply, with 80% of the total observations having ΔSSQ values less than 2,000 (Figure 9). For values of ΔSSQ greater than 2000 the observations begin to spread quite widely and reach values over 8,000 (Figure 9). These larger values are outliers on the right hand tail of the distribution of ΔSSQ, suggesting that the 182 light curves is enough observations to capture a reasonable representation of the tail of the distribution.

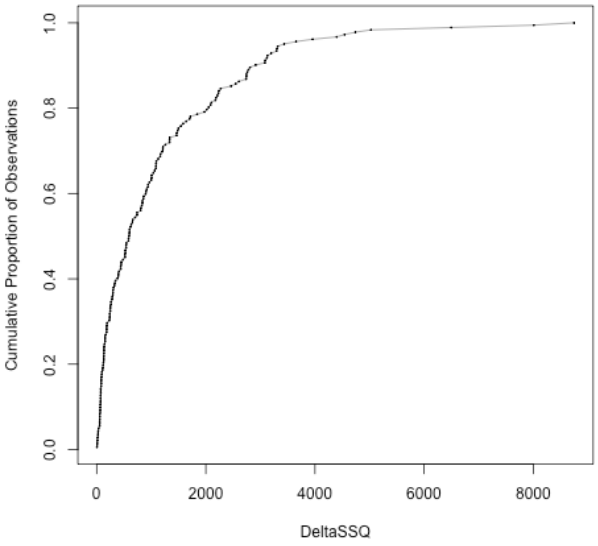

Figure 9. Cumulative density function for the distribution of the difference in sums of squares between predicted and observed light at the best fitting and true locations.

This cumulative density function for ΔSSQ was then used to convert a ΔSSQ value for any location and twilight observation, i.e. the difference in sums of squares for that location as compared to the location with the minimum sum of squares, into a relative likelihood using Wilke's theorem. This is essentially a rescaling of the differences in sums of squares, as can be seen by comparing the values of the sum of squares for a given light curve over the earth's surface with the relative likelihoods (Figure 10). Plotting the sums of squares for a single light curve across all possible locations one can see that there is a sigmoidally shaped band of relatively low sums of squares distributed in a north-south orientation on the planet surface (Figure 10). This band represents the locations where the light is changing in a manner most similar to that observed on the tag. Given that the tag is correctly identifying a twilight event, this band corresponds to the position of the twilight event on the earth's surface. The sigmoidal

shape is driven by the relative angle of the earth with respect to the sun and the curvature of the planet's surface.

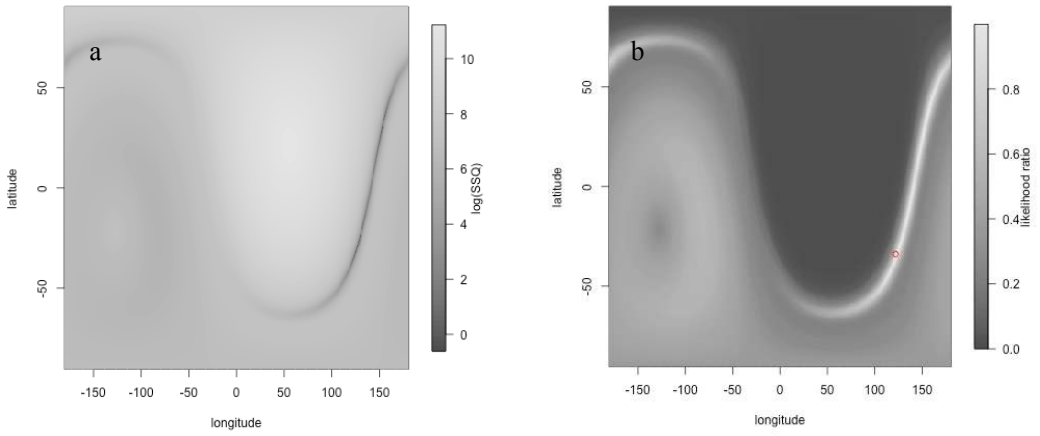

Figure 10. Relative fit of light data expected at locations around the earth in comparison with light observed at a single twilight event. Panel a) sum of squared differences between predicted light and observed light, b) relative likelihood from Wilkes theorem.

An important feature of the spatial distribution of the deviations is the distribution in areas far from the best fitting locations. The example shows the sum of squared deviations across the 11 light readings taken for the sunrise event on 12 January 2009 between 20:00:00 and 20:49:48 GMT (Figure 10a). As this is a sunrise event the area immediately to the left of the dark band, between longitudes 125 and -25 is night, while the area further to the left of longitude -25 is in daylight. One would expect locations equally distant from the true location at the same latitude to have similar deviations between the observed light and the predicted light. However, the deviations in these two regions differ markedly, with much larger deviations in the night time area than the daylight area. These areas differ in their deviations because the sun angle – light intensity relationship was only fit using the twilight data recovered from the mooring. Thus, predictions of light intensity for sun angles outside those observed around twilight events fall outside the fitted relationship (Figure 6) and are not well modelled.

With these patterns in mind it is possible to predict the uncertainty in location that will result from light based geolocation. It will be distributed along a sigmoidal shape, which will vary somewhat according to location and time of year. Importantly, due to uncertainty away from this ridge of higher values, the relative likelihood may not decrease in a symmetric way.

There is another important factor to consider in analysing light data from fish that dive on dawn and surface at dusk such as Swordfish and some of the tuna species. The diving behaviour of these fish can negate the effect of changes in sun angle on light intensity. The result is that although tags deployed on these fish may detect a twilight event and record data for it, that data can give very misleading estimates of location. In particular if the light levels recorded do not change by more than 40 to 60 units, the geolocation algorithm will have high certainty that the

fish is not located near a twilight event. Instead, the geolocation algorithm will have high certainty that the fish is in fact somewhere out in the region that is either dark or light at that time.

Given the potential for generating estimates of positions that are very certain and yet inaccurate when the light intensity data does not change adequately over the course of a twilight event, it was necessary to filter the light data included in the analysis to avoid this problem. Light data recorded by the tags varied from mooring data in three ways, all of which are relevant to the uncertainty that will result. First, light data recorded for some twilight events consisted of differing numbers of light readings. Mooring data processed by Wildlife Computers to simulate satellite tag data all had 11 light readings per twilight event. Light data from tags deployed on Swordfish ranged from 1 light reading to 11 light readings per twilight event. Second, the change in light intensity across twilight events also varied widely. The change in light intensity over a twilight event for the moored tag averaged 86 units. By contrast, the change in light intensity during a twilight event for tags deployed on Swordfish could range from similar values all the way to essentially no change. Finally, light intensity readings from tags deployed on fish occasionally did not change smoothly, but instead had variation over the course of the twilight event. In some cases this led to no change in light intensity over several readings, or even a reversal in the direction of change (e.g. an increase in intensity as night was coming on). The filter we used was based on two characteristics, light intensity changes of greater than 60 units over the course of the twilight event and a minimum of 6 light readings for the twilight event. Together these two criteria reduced the data set to light readings that resulted in position estimates that gave locations that generally coincided with the GPS estimates from the same tags.

7.4 STATISTICAL MODELLING OF MOVEMENT

The goal of the analysis of the tagging data from the Swordfish deployments was to a) develop an approach for evaluating whether fish showed evidence of seasonal migration, b) investigate retention times on the spawning grounds and in other regions if there was evidence for migration, c) to provide a succinct description of stock structure in the region, and d) to develop a model for movement that could be incorporated into other analyses. We addressed these goals by setting up a number of hypotheses about Swordfish behaviour in the region, which could then be posed as putative models and estimated in the hidden Markov modelling framework that we developed.

For all of the models in this section, the time interval is in days. After filtering the light data for dawn and dusk events that had at least 6 readings (out of 12 possible), and showed a change in light of more than 60 units, there were 37 useable dawn or dusk positions. These were combined with 62 GPS positions, 14 release locations, and 14 recovery locations to estimate the movement patterns across the tagged fish.

The effect of the distance between two successive locations is an important consideration in structuring the models that are to be analysed. The process that we are modelling is the probability that an animal chooses the next location where it is observed, given the last location where it was observed. Clearly one would expect that all other things being equal, locations that are further from the current location should be less likely to be chosen. There are at least two theoretical reasons for this assumption. First, if an animal moves a given distance from a location, a circle with radius equal to that distance intersects a larger number of cells on a regular

grid as the length of the radius increases. Thus given an animal is going to move a particular distance, there are more choices of possible locations as that distance increases. This would lead to each location having a lower probability of being chosen, even if all locations were equivalent in their attractiveness as a choice. Second, movement is energetically costly, and thus animals should minimize the distance they move subject to the availability of quality habitat at more proximal locations. Therefore, there should also be a negative effect of the distance from the current location on the probability of choosing a particular location.

We fit a base model that includes just the effect of the distance from the current location in predicting the probability of choosing a location at the next time interval. This model is a null model, in the sense that it is the most basic model that is theoretically reasonable (Gotelli and Graves 1996). The probability of choosing a particular location *j*, given an starting location *i* in this model is

$$\text{logit}\left(o_{ij}\right) = e^{-\alpha D_{ij}}. \tag{17}$$

The negative log likelihood for this model is 714, which gives an AIC of 1430 (Table A4.1, Zucchini and MacDonald 2009). For nested models, the minimum difference in AIC has to be greater than 2 for a more complex model to be considered significantly better (Burnham and Anderson 2002). Thus, the distance only model provides a basis for identifying more complex models that are better explanations of the underlying process of movement by Swordfish. The value of α in this model is 0.0025. The standard error of the estimate is 0.0009, which gives a 95% confidence interval of 0.0018 around the estimate for α, indicating that the distance effect is significant. In the model the distances are measured by the great circle distance (i.e. along the shortest line following the curvature of the earth) in kilometres. However, the estimate of α cannot be directly used outside the model to directly estimate the effect of a given number of kilometres on the probability a fish moves to a location. This is because when the transition matrix, Γ, is filled in each row has to be normalized to sum to one, as the rows represent the probability of moving to any location in the next unit of time. For instance, in the base model the probability of moving from grid cell 1, at (-45,145), to grid cell 2, at (-44,145), is 0.00144. However, the chance of moving an additional degree to the north is 0.00134, and moving two degrees to the north 0.00128. Thus, while it is possible to calculate the distance effect, they need to be normalized based on the dimension of the spatial grid used in the analysis to be appropriately scaled.

We explored the potential for differing preferences in the various regions of the Coral and Tasman Seas by fitting 3 models with increasingly detailed spatial blocking effects (Figure 3). The structure of the models was

$$\text{logit}\left(o_{ij}\right) = \beta_L L_j + e^{-\alpha D_{ij}}, \tag{18}$$

where β_L is the coefficient associated with spatial block L_j. The blocking effects in the models were numbered from south to north, working toward the largest block number in the northeastern corner of the analysis region (Figure 3). The first block (i.e. in the southwest corner of the region) was taken to be the reference block and always has a zero coefficient. Comparing the three models, each incorporating the distance effect from the base model, the AIC values were 1437.9, 1396.0, and 1390.0 for the 2 block, 4 block, and 8 block models respectively (Table A4.1). The coefficients for the spatial blocks are provided in Table 4. The fitting routine converged for these three models, however; it was not possible to estimate standard errors for

their parameters from the Hessian matrix. We instead used profile likelihoods, from which we were able to obtain 95% confidence bounds on some of the parameters (Table 4). For some of the parameters, we were still unable to obtain confidence intervals from the profile likelihoods, due to the flatness of the likelihood surface with respect to either upper, lower, or both bounds on the parameter (e.g. upper bounds on blocks 2 and 3 in the 4 block model, Table 4). This is likely due to the spatial coverage of the data. All of the spatial blocks in the model contained non-zero probability for at least some of the position estimates and thus should be estimable. However, in general the likelihood surface was flatter for parameters concerning blocks that were further from the locations with the most tagging data, and it is likely that the model is not very well constrained in that portion of the parameter space (Figure 3, Figure 5). Given this issue it is not possible to estimate the uncertainty around the parameter estimates to allow unambiguous comparisons across all parameters.

Table 4. Parameters for movement models including spatial blocks. Table layout shows the location of the blocks relative to Figure 3. Numbers in parentheses are 95% confidence intervals around the estimate. The subscript for on each estimate denotes the block identifier as described in the methods.

Spatial Blocking Design			
2 Blocks	4 Blocks	8 Blocks	
-0.42_2 (-0.42/-0.42)	-3.3_4 (-3.4/-3.3)	-93.1_4 (NA/NA)	-2.5_8 (NA/NA)
	12.7_3 (12.7/NA)	31.5_3 (NA/NA)	40.2_7 (NA/NA)
0_1	20.3_2 (5.7/NA)	32.1_2 (NA/NA)	8.3_6 (NA/NA)
	0_1	0_1	-3.0_5 (NA/NA)

However, the parameters suggest that the central portion of the analysis region is the preferred habitat for the fish. The block coefficients are lowest in the northern region (i.e. 4 in the 4 Block model, 4 and 8 in the 8 Block model), and northwestern corner is by far the least preferred. This is supported by the confidence intervals we were able to calculate in the 2 and 4 Block models. For instance, the lower bounds on the parameters for blocks 2 and 3 in the 4 block model exceed that for blocks 1 and 4. Again, as we were not able to calculate confidence intervals on all of the parameters this should be taken as a supportive result, but interpreted with some caution. Notably, the southeast corner of the region is also relatively less preferred (5 in the 8 Block model). This region has anecdotally been noted as having very large Swordfish caught outside of the spawning season, which assumed to be females migrating from the spawning ground (Robert Campbell, pers. comm.). The largest fish we tagged did in fact move in this direction from the tagging region in the centre of the spawning area (Figure 11).

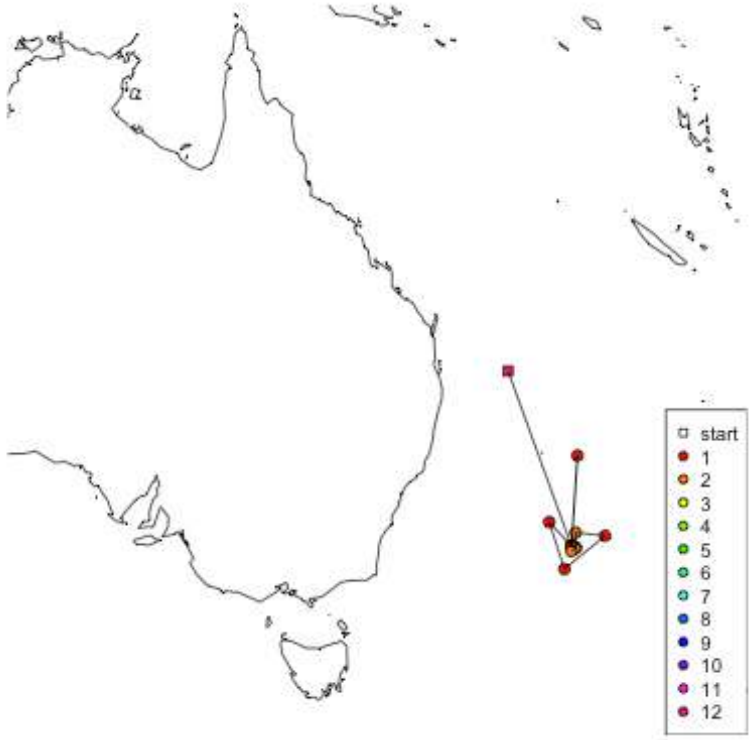

Figure 11. Southeastward movement by fish with tag id 84184.

We investigated the evidence for seasonal migration in movement by comparing spatially structured models that did not include a seasonal shift in the attractiveness of different spatial areas with a second set of models that had the possibility of allowing a seasonal change in attractiveness. This was achieved by incorporating a season effect in the model terms in (15). Thus the equation for the model without a seasonal effect is as in (18) above. The model including the spatial block and seasonal term is similar, but with an additional term for the interaction between the S_t and the location L_j,

$$\text{logit}(o_{ij}) = \beta_L L_j + \beta_{SL} L_j S_t + e^{-\alpha D_{ij}}. \quad (19)$$

Given the difficulty in estimating standard errors in the more complex models above with either 4 or 8 spatial blocks, we only present the results for (19) using a two block spatial structure. There is no main effect for season in this case; it only appears as an interaction term with the location. The AIC for the more complex model, including a seasonal interaction term and a spatial term is 1418.0, while the value for the reduced model including only the spatial effect is 1437.9 (Table A4.1). Thus the more complex model significantly improves the fit of the model over the simpler version. Notably, the model with the seasonal interaction also fits the data better than the null model. These results indicate that there are seasonal differences in the preference of Swordfish for the northern versus southern parts of the habitat, and that the inclusion of this effect is an overall improvement on the process model.

The spatial blocking in this model is divided into a northern and a southern block (Figure 3, left panel). The southern block effect has a coefficient of 0 for its main effect, and an interaction term coefficient of -5.93 with confidence interval of 8.02 (Table A4.1). The northern block has a coefficient of 3.53, however, the model fitting algorithm was unable to estimate a standard error for the term. The northern interaction term was -9.72 with a 95% confidence interval of 5.79. The distance effect, α, was -0.002 with a 95% confidence interval of 0.00092. These results suggest that in the nonspawning season the animals are more likely to move to locations in the northern region than to the southern region (i.e. 3.53 vs. 0). In the spawning season, summing the interaction term and the main effect, the coefficient for the southern region is -5.93, while that for the northern region is -6.19. This suggests that the attractiveness of locations in the northern region is less than the southern region during the spawning period. This pattern can be seen in the distribution of the fish in the two seasons (Figure 12). In the spawning season, fish are widely distributed throughout the region, and movements occur in both the northern and southern blocks (Figure 12a). However, as the season progresses fish increasingly move southward.

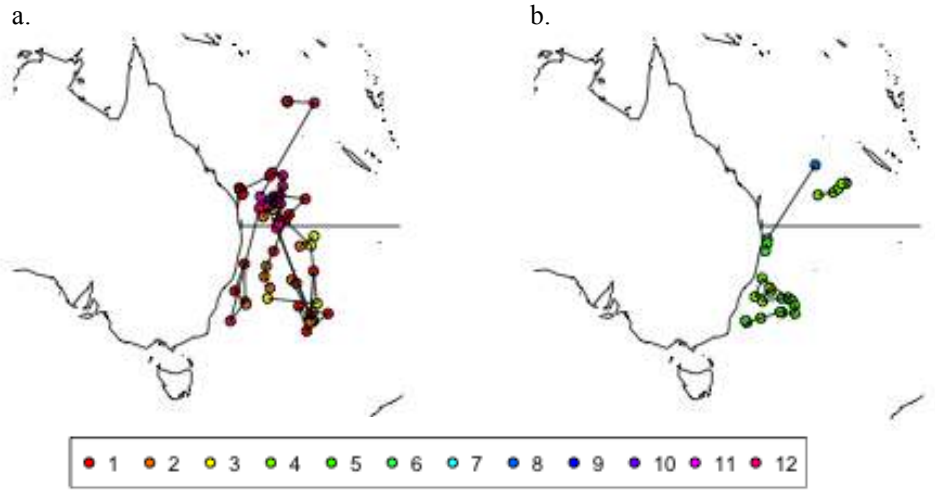

Figure 12. Locations of tagged fish in the spawning season. Panel a) during the spawning season, b) outside the spawning season. The horizontal line shows the spatial block boundary. The colours correspond to the month the location was recorded.

Outside the spawning season most of the records are in the southern block, thus most of the locations chosen by fish are also in the southern block. One fish does move northward in the non-spawning season; however, there is only one location in the track in the northern block (Figure 12b). Given the relatively large number of positions in the southern block, this one movement is not enough to create an interaction term. Thus the model does provide sensible results given the data.

While it would be possible to use more complex spatial structures than the two block division, we restricted the analysis to a spatial factor with two blocks. The primary reason is that for models with more complex spatial blocking patterns we were not able to get estimates of the standard errors for the coefficients. Incorporating a seasonal interaction term as in (19) more than doubles

the number of parameters required for a model. This increase is likely to make the estimation of standard errors even more difficult, and thus we did not extend the model. It is possible that with additional data this problem could be resolved. An alternative would be to try a different parameterization for the spatial structure, which might also resolve the issue.

In order to understand residence times of Swordfish in the Coral and Tasman Seas we also evaluated the role of site fidelity, or philopatry, in structuring movement patterns of Swordfish. One issue that arises in trying to understand philopatry is how to structure hypotheses in order to test for it. It is possible to use measures like the relationship between net displacement and time to test for philopatry using raw position data, as in 7.2. However, it is not easy to incorporate uncertainty in location estimates in this approach. In addition, the analysis of maximum displacements with time also only uses the starting and ending points, ignoring other positions. An alternative is to include a philopatry effect in the state space model and evaluate its effect across all of the observations that have been made for each fish. We incorporated a measure of philopatry by including the distance from the initial tagging site as a covariate determining the attractiveness of each spatial location to which a fish could move. This effect was included in the first term of the linear model for the movement probability from location *i* to location *j* as

$$\text{logit}\left(o_{ijk}\right)=\beta_{\delta}\delta_{jk}+e^{-\alpha D_{ij}}, \tag{20}$$

where δ_{jk} is the distance in kilometres from the initial tagging location for fish *k* to location *j*.

This model was compared against the base model that only has a distance effect between successive positions (17). The AIC for the model including the distance from the starting location is 1263.6 (Table A4.1). This is substantially lower than the AIC for the base model of 1430, and also much lower than the model including a block effect, with or without spawning. Both of the parameters are significantly different from zero. The parameter estimate for α is 0.0044 with a 95% confidence interval of +/- 0.0032. The estimate for β_{δ}, the coefficient for the distance from the start, is -0.0034 with a 95% confidence interval of +/-0.00053. Based on these estimates, fish are less likely to choose locations that are far from their current position, and, even controlling for this effect, fish are less likely to choose locations that are far from the location where they were tagged.

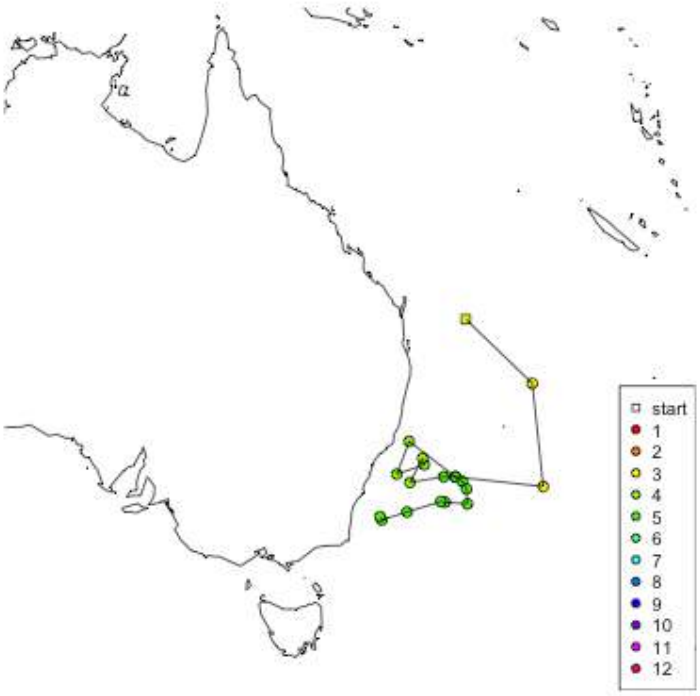

Figure 13. Locations over the months of the year for the fish with tag 39969.

The location where a fish is tagged is representative of its location preference. If fish show philopatry, their tagging location should be within the region they prefer. In fact one would expect the chance of catching a fish in a location to be directly proportional to its preference for that location. The significant negative coefficient for the effect of distance from this location on the attractiveness of potential future locations indicates that the Swordfish off the east coast of Australia do have strong philopatry.

However, this philopatry may be relevant at a range of scales. Fish with a spawning migration will show philopatry if tagging data covers a long enough period for them to reach locations where they spend significant amounts of time. For instance, the fish with tag 39969 was tagged due east of Fraser Island, over the course of the next month it moved south, and then spent a period of time near the continental shelf off southern New South Wales. While this fish is not returning to the location at which it was tagged, the total displacement from the tagging location is much less than the minimum linear distance the fish has moved (Figure 13).

The parameter estimate for β_δ gives a measure of the scale at which this philopatry occurs and could be used to calculate the probability of a given fish remaining inside an area of any given size. For instance, assuming a tagging location and a current position for a hypothetical fish, we can use (20) to calculate the probability of moving to any other location on a grid covering the Tasman and Coral Sea region (Figure 14).

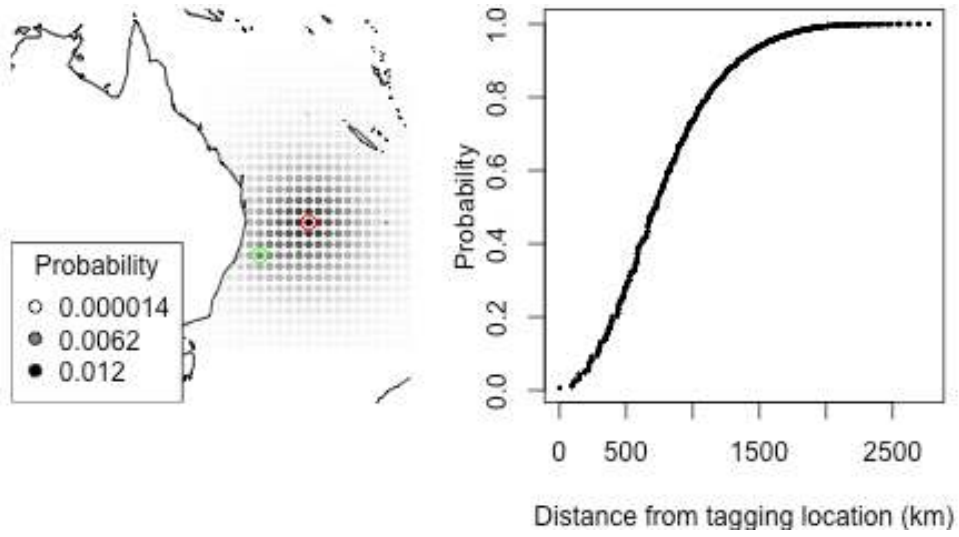

Figure 14. Movement probabilities for a fish in the next day. Panel a. Estimated movement probabilities plotted on a 1 degree by 1 degree grid. The starting location has a green outline (155, -32), tagging location has a red outline (160,-29). Panel b. Cumulative probability of moving to a location with distance from the initial tagging location. Probabilities are calculated using (20) and the fitted values presented above, as explained in section 6.2.4. Shaded points are plotted on a 1 degree by 1 degree grid.

Visualizing the pattern for a hypothetical fish (Figure 14), one can see that the effect of philpatry is fairly strong in comparison with the effect of the distance from the fish's current location, as would be expected from the parameter estimates. Locations nearest the position where the fish was initially tagged are much more probable than even positions adjoining the current location of the fish, highlighted in green (Figure 14). Similarly, the upper and lower confidence intervals for the parameters in (20) can be used to quantify the uncertainty around these estimates of movement probabilities, and if desired to simulate movement patterns while including uncertainty. Examining the cumulative probabilities of moving to a location, sorted by distance from the starting location indicates that there is a probability of 0.2 that the fish will move back to within 400 km of its original tagging location in the next day, although it is currently 583 km away (Figure 14b). This consistent bias in movement back toward the original tagging location will result in a relatively restricted distribution, as given any move away from the original tagging location there is a strong bias back toward it. For instance, for the hypothetical fish in Figure 14, comparing the probabilities of a move to the next location to the southwest of the current location to that for a move to the location on position immediately to the northeast of the tagging site, there is a much higher probability to move to the second position even though it requires a much longer movement. It is important to note that the movement probabilities are dependent on both the current location, and the tagging location, thus in using these results the probability distribution needs to be calculated for each position sequentially.

Applying the state space model developed in this project to the tagging data from Swordfish in the Coral and Tasman Seas, we have demonstrated spatial variation in habitat preference, a seasonal migration pattern, and evidence for philopatry. The estimated parameters from these models can be used explicitly in calculating mixing ratios for specific cases of interest. The

transition matrix, Γ, gives the probabilities of moving from one location to another, based on the parameter estimates for the linear terms which determine its component probabilities (Figure 14). In the current application the time step for the matrix is a daily one, and the matrix is implemented on a one degree grid. However, all probability calculations are done on great circle distances calculated in kilometres. Thus estimation of potential movement patterns for a single fish, or even a population of fish, can be done straightforwardly by simulating from this matrix. It would also be possible to calculate other quantities from the transition matrix, such as the time to move from one location to another or the fraction of animals moving from one location to another.

One word of caution applies in simulating from the estimated parameters however. The parameters in this analysis are based on tagging data from the Coral and Tasman Seas region. If the simulation is applied outside that region, it will be dependent on the animals exhibiting similar behaviours. However, incorporating additional data would provide the possibility of extending the area of relevance of the model.

8. BENEFITS

The tagging data described in this report adds to the developing library of data on the movement and behaviour of pelagic species in the Australian region. In particular the development of towed tags incorporating GPS sensors has substantially increased the quality of the available information on the behaviour and movement of Swordfish in the region (Evans et al. 2011). These tags were developed by Wildlife Computers, in collaboration with project staff and CSIRO's marine engineering staff in Hobart. Historically, data from tags using light-based geolocation were very difficult to analyse due to the large and uncertain error associated with their positions. Lab and field trials, with subsequent operational deployment of these GPS enabled tags significantly increased the quality of the data available for this project and subsequent users of the data.

Information on Swordfish movement from Swordfish tagging data provided important insight for the regional WCPFC stock assessments in 2008 and 2013, and evaluation of the domestic Australian Eastern Tuna and Billfish longline Harvest Strategy (Kolody et al. 2008, Kolody et al. 2010, Davies et al. 2013). There were not enough tag releases with sufficient spatial coverage and time at liberty to provide definitive estimates of stock structure and mixing rates. However, particularly when combined with the tagging information from international collaborators, the tags were sufficiently informative to plausibly bound the population connectivity assumptions and ensure that this key uncertainty was adequately represented (Kolody D. pers. comm).

The analysis tools developed in this project provide a number of benefits. First, the development of an algorithm for estimating the uncertainty around light based positions provides a unique opportunity to be able to incorporate these position estimates into statistically robust models. Prior to this advancement, none of the analytical methods available could provide estimates for positions from light data that were independent of each other. Due to this limitation it was not possible to analyse them in a statistically robust manner. Second, development of these uncertainty estimates has allowed the integration of several dissimilar data types into a single analysis. Again in the absence of the uncertainty estimates this had heretofore been impossible.

Third, the development of a state space model for animal behaviour which is appropriate for the temporally intermittent data typical of species like Swordfish has opened a new door in terms of investigating the behaviour and distribution of these species. Using this model it is possible to investigate questions such as large-scale habitat preferences, mixing rates across adjoining areas, and to quantify the seasonal characteristics of their movement.

In terms of management application this report not only provides estimates of the scale and pattern of movement and habitat preferences, but also a basis for incorporating these estimates into other models in a readily usable form. The estimates from the analysis can be incorporated directly into models of population dynamics, catch availability, and mixing ratio by using the estimates provided and the appropriate spatial structure to implement a transition matrix based on (17), (18), (19), or (20). Recent assessments, which used electronic tag data to inform mixing rates, utilized relatively simple models based on diffusion approximations (Kolody et al. 2008, Evans et al. 2012). The analytical model developed here can accommodate some of the complexities that were noted in this analysis, which were difficult to incorporate (Evans et al. 2012). In fact, the hidden Markov model developed in this report directly addresses the need identified for analytical tools to handle tagging data in support of future Swordfish assessments (Evans et al. 2012). There is an ongoing update to the harvest strategy for Swordfish (FRDC project 2013/203), and the final report from this project has been provided to the project team in the event that it may prove useful.

Ultimately the information in the report should support the ongoing management of the Swordfish. The evidence for philopatry confirms the hypothesis that was formed in the late 1990s when serial depletion was documented around seamounts off the east coast of Australia (Campbell and Hobday 2003). Swordfish do in fact appear to be a relatively distinct local population segment, with limited mixing outside the Coral and Tasman Seas. This does not necessarily imply a genetically distinct stock, but instead that individual fish show philopatry, which is likely to reduce mixing, rates at larger scales. While it is unclear if this pattern extends to regions beyond the Coral and Tasman Seas based on the data presented here, descriptive analysis of a larger dataset covering the South Pacific does seem to support this general pattern of reduced mixing at large scales (Evans et al. 2014).

The Ministerial directive issued to AFMA in 2005 urged the Authority to consider spatial management for Commonwealth fisheries where appropriate. The Eastern Tuna and Billfish Fishery was briefly managed using an effort management system that was proposed to include spatial management, coinciding with the development of this project. Consideration of spatial management faded however, as the fishery moved to output quota management in 2010. If spatial management is considered as an option in the future, the models presented in this project could be used directly to estimate the expected reduction in exposure to fishing mortality resulting from a closure or other spatial control of any given size by considering the expected residency in the restricted area. While no specific predictions were provided for management scenarios in this project, the results presented would allow direct calculation of management area temporal coverage.

9. FURTHER DEVELOPMENT

There are a number of extensions that could be developed to the existing analysis model, including incorporation of GPS uncertainty, and addition of random and fixed effects to understand the difference among individuals. Another extension that could prove fruitful would be the incorporation of additional data in estimating location errors, in particular for light-based locations. It would be possible to utilize information on sea surface temperature and potentially depth in inferring positions. However, it is unclear how much this additional information would reduce the uncertainty given the relatively limited movement of the fish. The model in its current implementation is relatively time consuming to estimate for more than a few parameters. More extensive use of the approach would benefit from migration to a more efficient estimation framework, such as the analytical derivatives available in ADMB (admb-project.org). An alternative would be to recode some of the slower portions of the model to optimize their speed in the current framework.

The analysis could also benefit from the incorporation of additional data. There has been substantial data collected on Swordfish in the southern Pacific Ocean since the initiation of this project (e.g. Evans et al. 2014). As this data becomes available, it would be possible to revisit the analysis. Additional data would likely provide better estimates in the model. In particular more spatial coverage of the Coral and Tasman Sea region would improve estimates for spatial blocking effects and likely improve estimates of the confidence intervals on their parameters. Inclusion of additional data would also facilitate more complex models including fish characteristics such as size or weight. Incorporation of data from the regions of the Pacific further east would facilitate extending the spatial structure in the model. This would allow closer evaluation of mixing between the Coral and Tasman Seas and adjoining regions to the east.

Electronic tagging data collected in this project is held in a devoted database housed on a central server and backed up daily at the CSIRO Marine and Atmospheric Research Division in Hobart, Tasmania. The database includes facilities for data upload, quality checking, handling, and delivery. The database is password protected. Data summaries are available through the project Principal Investigator. Provision of raw or processed data will be considered for collaborative research projects. Statistical code is also available for collaborative projects. Ongoing upload of legacy data, quality control and analysis will proceed in the future.

10. PLANNED OUTCOMES

The planned outcomes from project proposal were as follows: “This project will directly investigate the connections between the Swordfish population spawning in the Coral Sea, the section of that spawning population that is harvested by the Australian fishery, and the movement of fish from the Coral Sea spawning region into the western/central Pacific using movement paths provided by pop-up satellite archival tags. The primary outcome will be succinct quantitative description of stock structure and movement that can be used as a basis for developing harvesting strategies and spatial management for an internationally shared stock. The resulting movement model and analysis will address the needs outlined in the Need and Background sections as follows: 1) it will provide estimates of movement rates between regions, helping clarify a fundamental uncertainty in the ongoing and future Swordfish assessments in the region; 2) it will underpin a quantitative basis for developing a domestic and international harvest strategy, and

advocating that policy into the WCPFC, the regional RFMO for the Southwestern Pacific; 3) information resulting from it will assist in designing spatial management for the ETBF, and addressing the ongoing localized depletion in the fishery. These benefits will accrue primarily to the industry in terms of a more robust and reliable basis for management and advocacy by AFMA and DAFF, leading to increased management certainty."

The movement model for Swordfish was developed as proposed, and provides a quantitative description of movement. Swordfish movements were much more limited than had historically been suspected, with fish tagged in the Coral and Tasman Seas remaining within the basin. Thus the outcomes of the modelling and analysis focus largely on site fidelity, as opposed to stock structure as there was no connectivity with stocks to the east of New Zealand and New Caledonia observed from tags deployed in this project. In terms of the specific outcomes proposed for the project listed in the proposal, we were able to estimate movement rates within the region Tasman and Coral Seas, but not outside due to limited movements by tagged fish. Tag data from this project and others have been used in developing assessments for Swordfish in the Southwestern Pacific region. This project has provided results as planned that could be used directly in designing spatial management, if that need arises. As outlined in Section 8, management in Australia's Swordfish fishery has moved away from spatial management of effort toward catch quota management during the life of this project. However, as spatial depletion has been observed in the past both domestically and elsewhere, it is certainly possible that the need for spatial management will arise again.

Outreach and promotion of the project findings will be ongoing for the next two years. Project results were presented to researchers and managers involved in international tuna and billfish management at annual meetings sponsored by the IATTC in 209, 2010, 2011, and 2012. The final report will be presented to the TTMAC and TTRAG during a future meeting, to be scheduled in 2014 dependent on availability of time during upcoming meetings. Two publications are in preparation from the project, the first covering the analysis method entitled "Analyzing sparse tagging data using hidden Markov models – a discrete choice approach" and a second focusing on Swordfish movement patterns and site fidelity entitled "A comparison of the influence of site fidelity and habitat suitability on movements of large pelagic fish". Press releases will be prepared and promoted by CSIRO communications staff, when the publications are due to appear. A summary of the final report will be prepared as a paper for the Western Central Pacific Fisheries Commission, and provided as a paper to their scientific meeting. Final report copies will be provided directly to all co-authors on the 2008 and 2013 Swordfish stock assessments, along with the project team currently leading the update of harvest strategies for pelagic species funded by the FRDC (project 2013/203).

11. CONCLUSION

The project was able to achieve all of its objectives, with the exception of incorporation of data sets collected by other researchers. These data sets were not available in time to be included in the analysis, and thus did not form part of the results. As these data become available they could be included with the project data and reanalysed. The analysis tools designed in this project are relatively modular, and would easily accommodate new tagging information.

In term of the proposed outputs, the analysis presented here demonstrates that Swordfish in the Australian region are likely mixing in only a relatively limited way with stocks further to the east. There is very strong evidence for site fidelity, or philopatry, which is easily visible in plots of the locations reported from the tagged animals. This philopatry occurs at a number of scales. At the very largest scale it is a result of a likely spawning migration pattern, which sees the fish shifting locations within a bounded region over the course of a year. At a smaller scale it is likely related to site fidelity around seamounts and along the continental shelf, which may be a function of the foraging preferences of individual fish.

The analysis was done in a framework that should make it relatively straightforward to incorporate into other analyses of stock structure, mixing rates, and population dynamics. Estimated coefficients for the necessary terms were provided, along with estimates of their uncertainty. In order to support potential uptake of the project results, the discussion section included an example implementation of the model to estimate mixing as would be done in the context of either population modelling or analysis of spatial management.

REFERENCES

Burnham, K. and D.R. Anderson. 2002. Model selection and multimodel inference: a practical information theoretic approach. Springer, New York, USA. ISBN 9780387953649. 488 pp.

Campbell, Robert. CSIRO Marine and Atmospheric Research, Hobart, Tasmania, Australia.

Davies, N., G. Pilling, S. Harley, and J. Hampton. 2013. Stock assessment of swordfish (Xiphias glades) in the Southwest Pacific Ocean Secretariat of the Pacific Community, Oceanic Fisheries Program Pohnpei, Federated States of Micronesia

Evans, K. 2010. Investigation of local movement and regional migration behaviour of broadbill swordfish targeted by the Eastern Tuna and Billfish Fishery. CSIRO Marine and Atmospheric Research. Hobart, Tasmania, Australia. ISBN 9781921605840. 94 pp.

Evans, K., H. Baer, E. Bryant, M. Holland, T. Rupley, and C. Wilcox. 2011. Resolving estimation of movement in a vertically migrating pelagic fish: Does GPS provide a solution? Journal of Experimental Marine Biology and Ecology 398:9-17.

Evans, K., D. Kolody, F. Abascal, J. Holdsworth, P. Maru, and T. Sippel. 2012. Spatial Dynamics of Swordfish in the South Pacific Ocean Inferred from Tagging Data Western and Central Pacific Fisheries Commission, Kolonia, Pohnpei, Federated States of Micronesia.

Evans, K., F. Abascal, D. Kolody, T. Sippel, J. Holdsworth, and P. Maru. 2014. The horizontal and vertical dynamics of swordfish in the South Pacific Ocean. Journal of Experimental Marine Biology and Ecology 450:55-67.

Gottelli and Graves 1996. Null models in ecology. Smithsonian Press. Washington D.C., USA. ISBN 978-1560986577. 368 pp.

Kolody, Dale. CSIRO Marine and Atmospheric Research, Hobart, Tasmania, Australia.

Kolody, D., R. Campbell, and N. Davies. 2008. South-West Pacific swordfish (Xiphias gladius) stock assessment 1952 - 2007. CSIRO Marine and Atmospheric Division, Hobart, Tasmania.

Kolody, D. S., A. L. Preece, C. R. Davies, J. R. Hartog, and N. A. Dowling. 2010. Integrated evaluation of management strategies for tropical multi-species long-line fisheries. CSIRO Marine and Atmospheric Research, Hobart, Tasmania.

Meenus, J. 1998. Astronomical Algorithms, 2nd edition. Willmann-Bell. Richmond, Virginia, USA. ISBN 978-0943396613. 477 pp.

Patterson, T.A., Thomas, L., Wilcox, C., Ovaskainen, O. and Matthiopoulos, J. 2008. State space models of individual animal movement. Trends in Ecology and Evolution. 23:87-94.

R Development Core Team (2010). R: A language and environment for statistical computing. R Foundation for Statistical Computing, Vienna, Austria. ISBN 3-900051-07-0, URL http://www.R-project.org.

Reeb, C. A., L. Arcangeli, and B. A. Block. 2000. Structure and migration corridors in Pacific populations of the Swordfish Xiphius gladius, as inferred through analyses of mitochondrial DNA. Marine Biology 136:1123-1131.

Turchin, P. 1998. Quantitative Analysis of Movement. Sinauer . USA.pp 396.

Young, J. and A. Drake. 2002. Reproductive dynamics of broadbill swordfish (Xiphias gladius) in the domestic longline fishery off eastern Australia. CSIRO Marine and Atmospheric Research, Hobart, Tasmania, Australia. ISBN 1-876996 23 4. 121 pp.

Zucchini W. and I.L. MacDonald. 2009. Hidden Markov models for time series: an introduction using R. CRC press. London, United Kingdom. ISBN 978-1-58488-573-3. 275pp.

APPENDIX 1. INTELLECTUAL PROPERTY

The tagging database that houses the electronic tagging data from this project was developed in a range of projects fully or partially funded by CSIRO, and remains the property of those projects as specified by the intellectual property agreements in those projects. A number of methods and datasets using in the tagging analysis methods and geolocation methods in this project were developed in part in other external and internally funded projects at CSIRO. These methods and data remain the property of those projects, and their use is governed by the intellectual property arrangements specified in those projects.

APPENDIX 2. STAFF

Chris Wilcox, Principal Investigator, Data Analysis

Karen Evans, Logistical Support, Data Entry

Matt Lansdell, CSIRO, Logistical Support, Fieldwork

APPENDIX 3. PLOTS OF MOVEMENTS BY TAGGED FISH

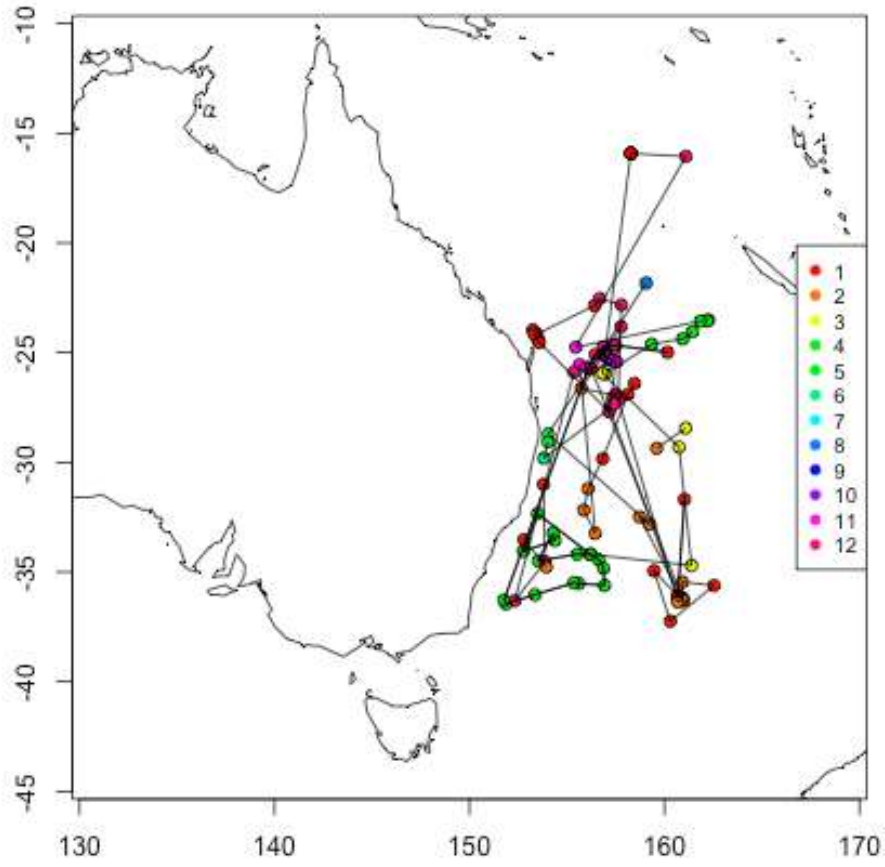

Figure A3. 1. Map of all tag locations for tags deployed in this study. Legend colours show months during which locations were recorded.

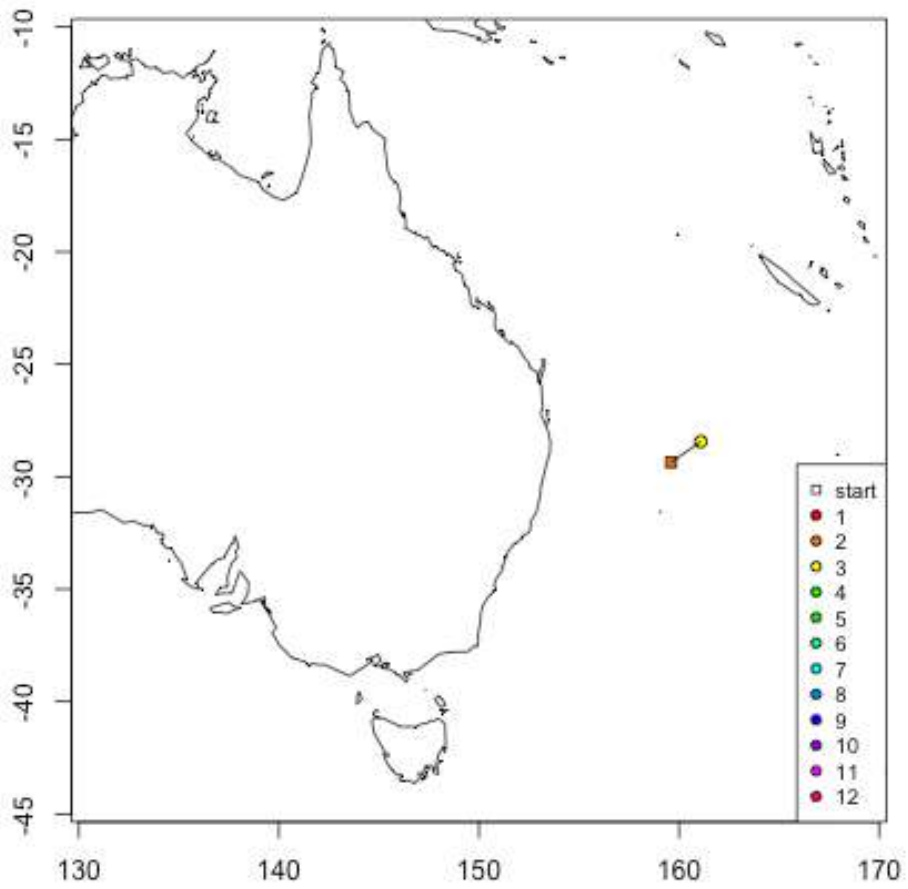

Figure A3. 2. Map of the locations reported by tag 36861. Legend shows starting location and locations over the tag deployment period coloured by month.

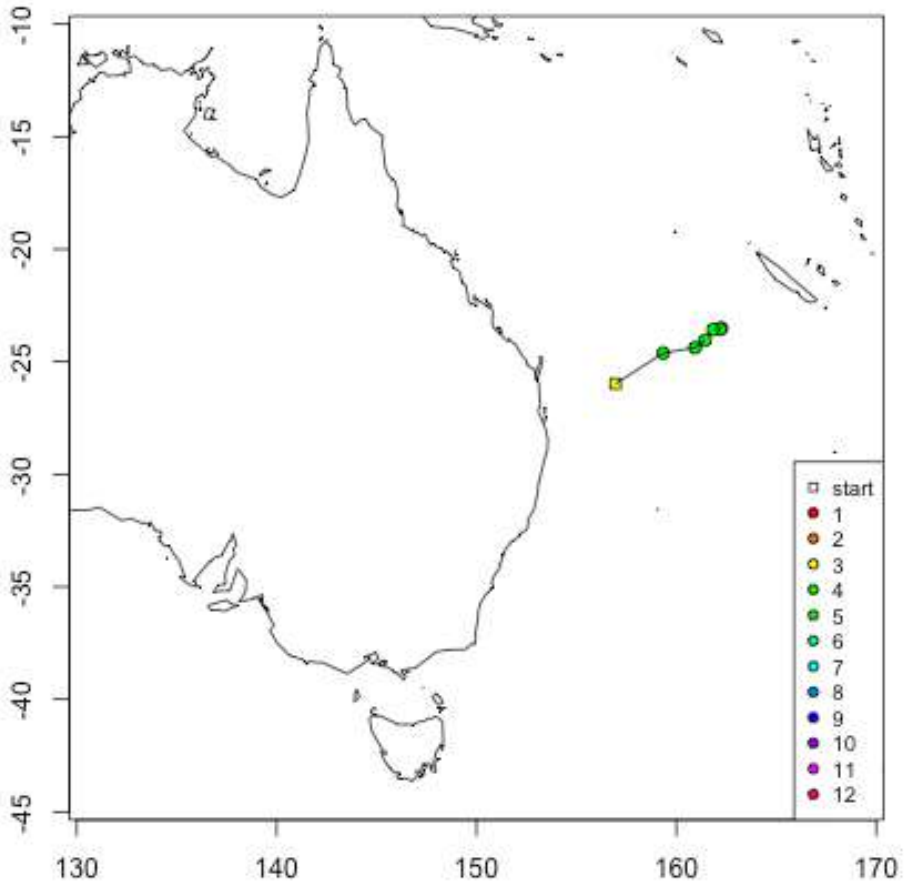

Figure A3. 3. Map of locations reported by tag 37702. Legend shows starting location and locations over the tag deployment period coloured by month.

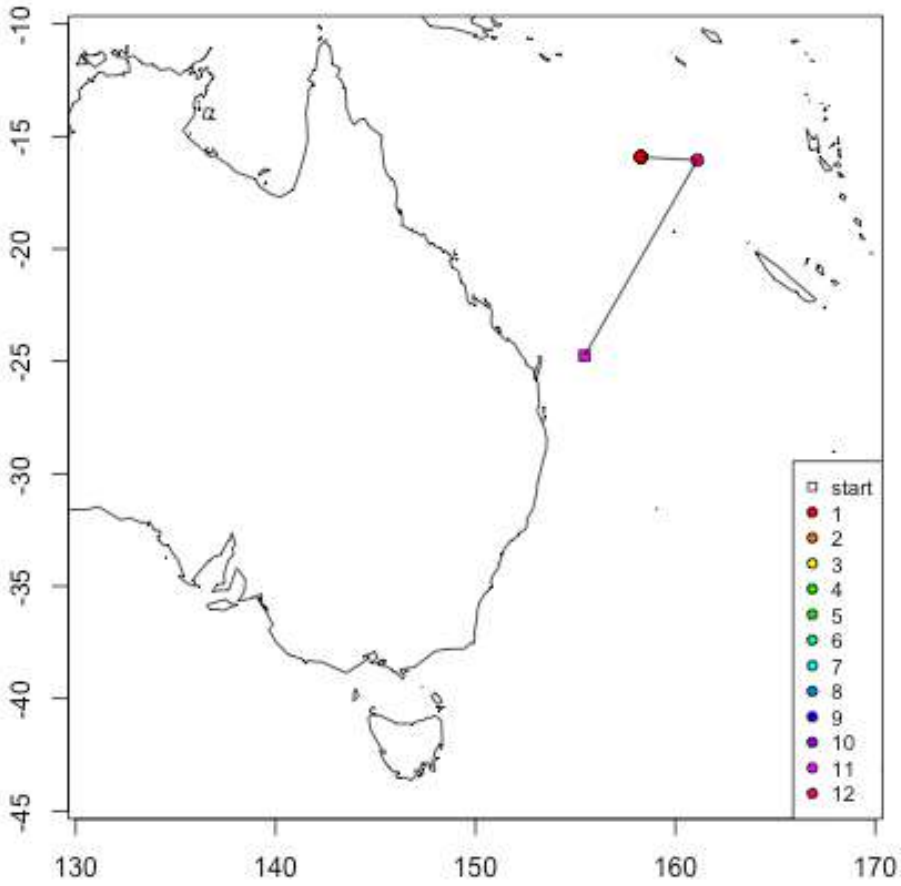

Figure A3. 4. Map of locations reported by tag 39796. Legend shows starting location and locations over the tag deployment period coloured by month.

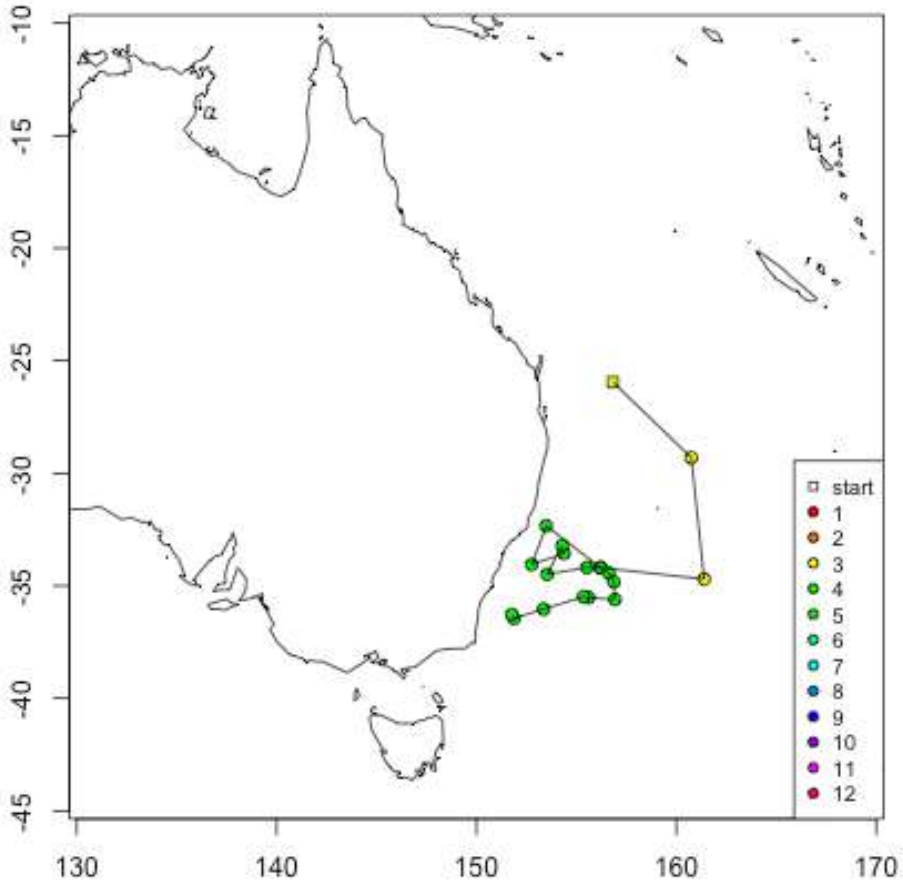

Figure A3. 5. Map of locations reported by tag 39969. Legend shows starting location and locations over the tag deployment period coloured by month.

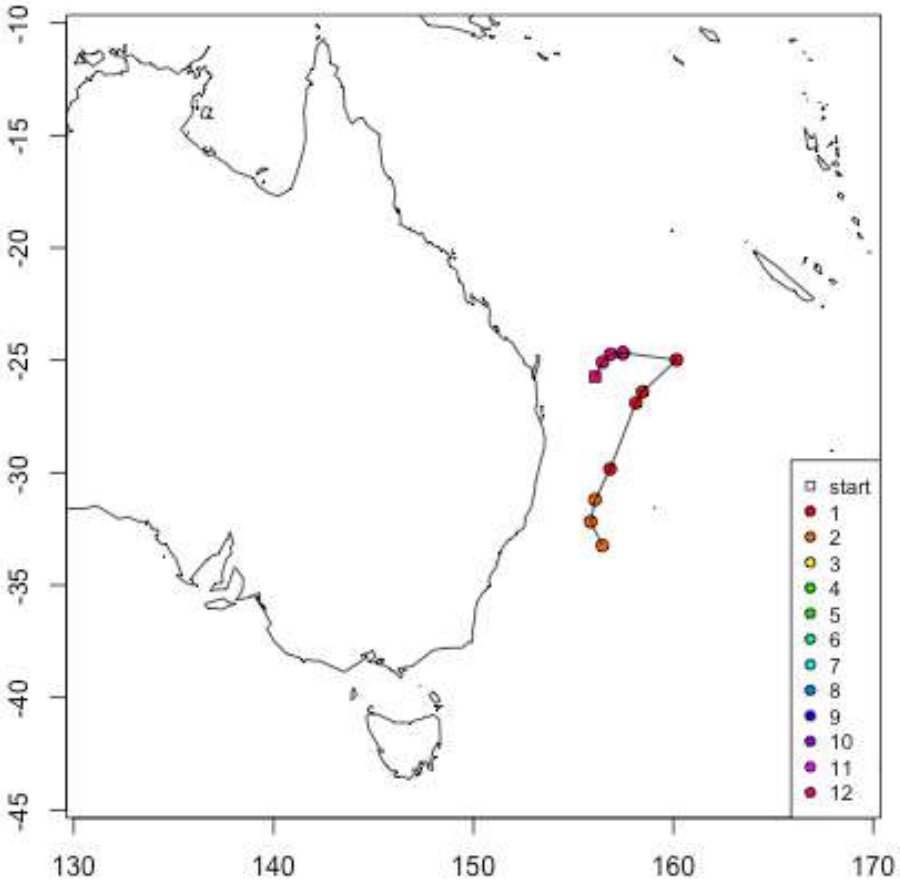

Figure A3. 6. Map of the locations recorded by tag 39970. Legend shows the starting location and all locations recorded by the tag coloured by month.

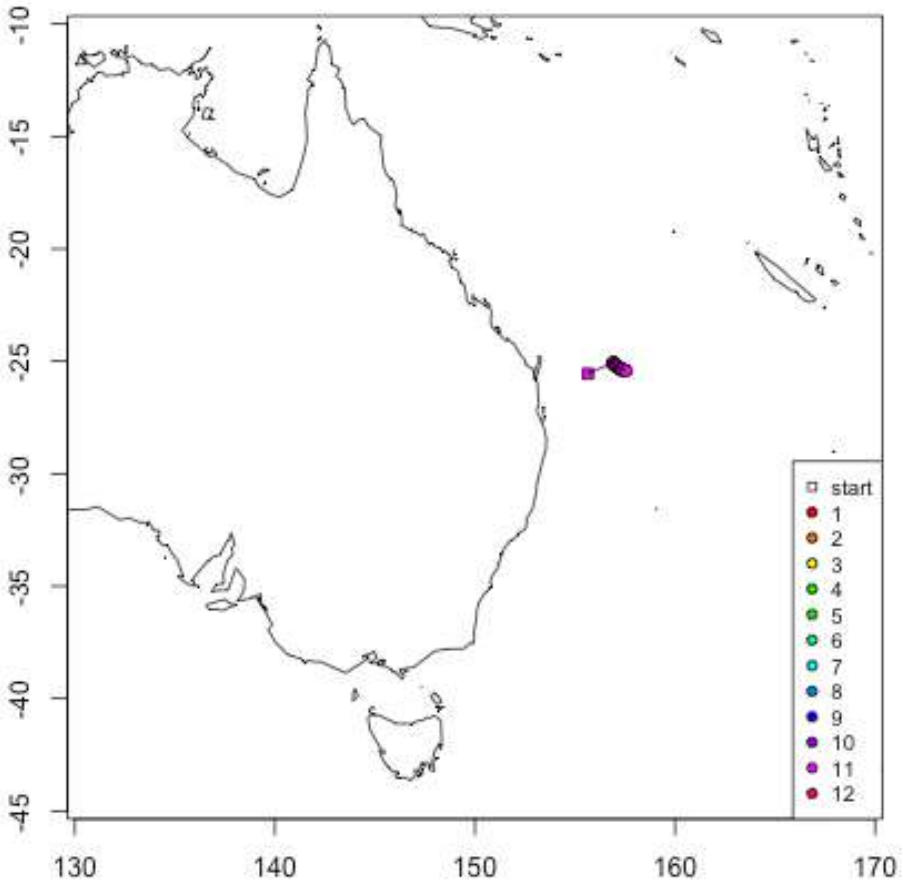

Figure A3. 7. Map of the locations recorded by tag 83860. Legend shows the starting location and all locations recorded by the tag coloured by month.

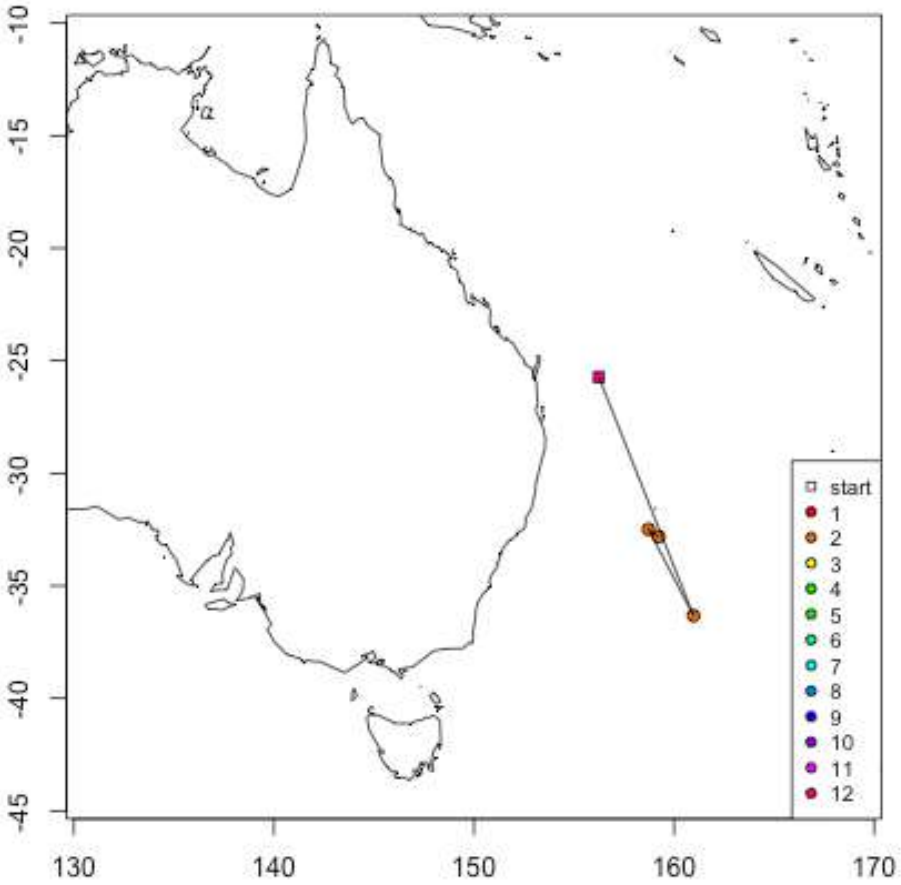

Figure A3. 8. Map of the locations recorded by tag 83861. Legend shows the starting location and all locations recorded by the tag coloured by month.

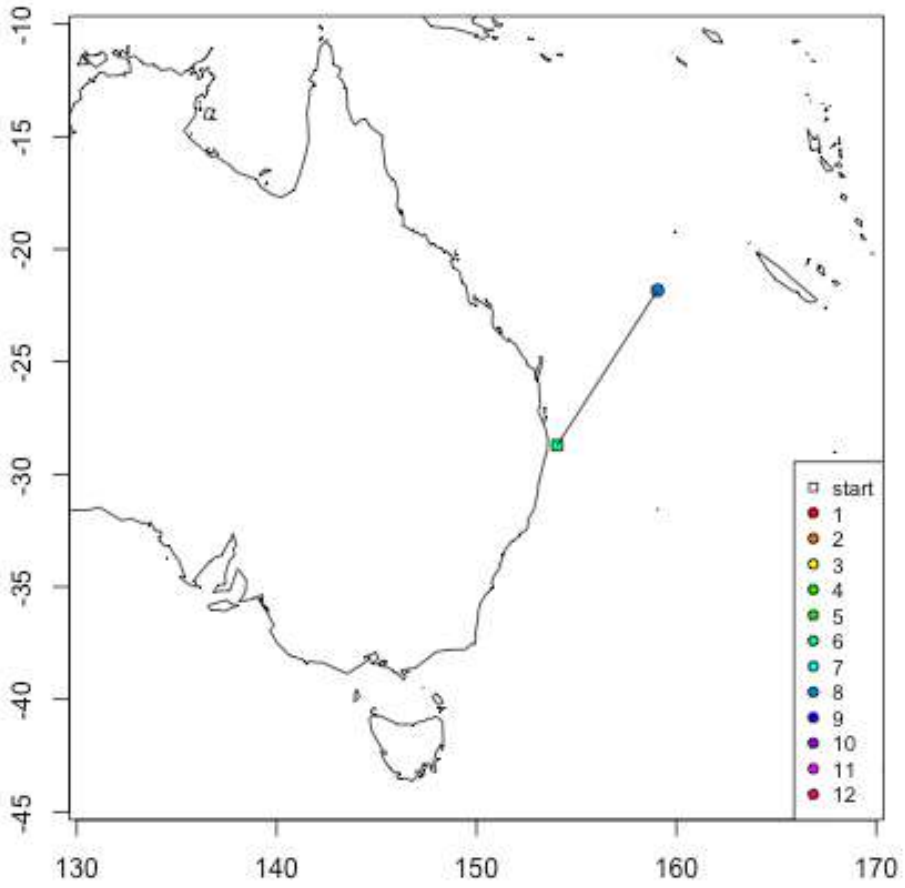

Figure A3. 9. Map of the locations recorded by tag 83862. Legend shows the starting location and all locations recorded by the tag coloured by month.

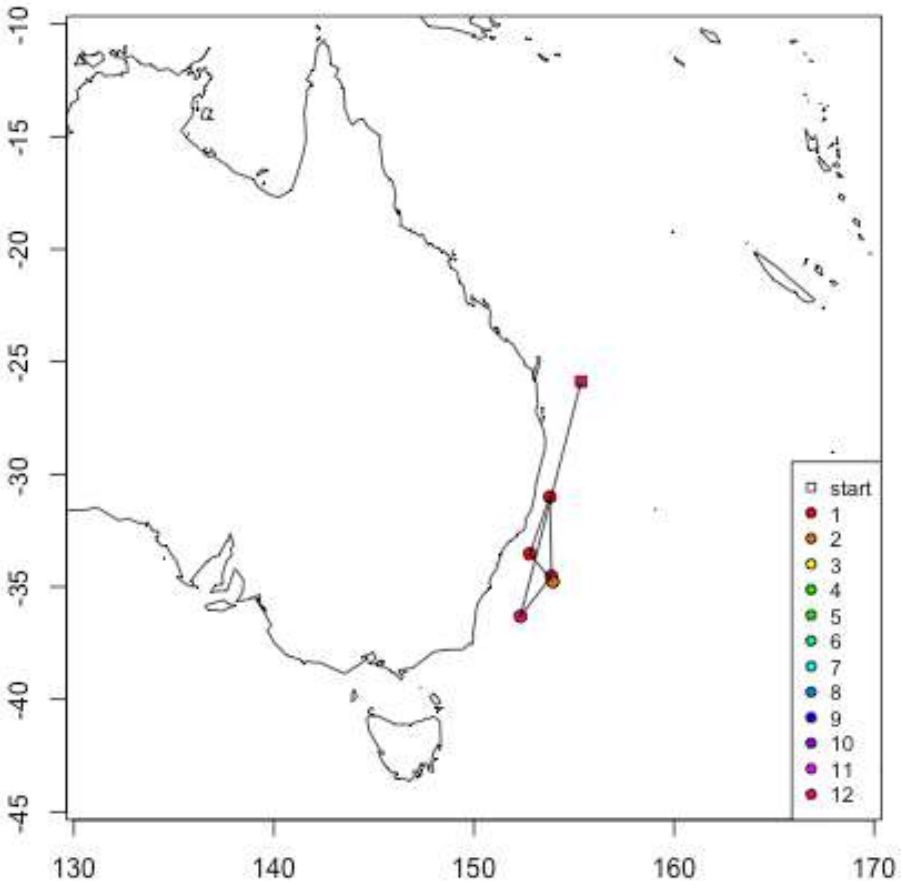

Figure A3. 10. Map of the locations recorded by tag 83863. Legend shows the starting location and all locations recorded by the tag coloured by month.

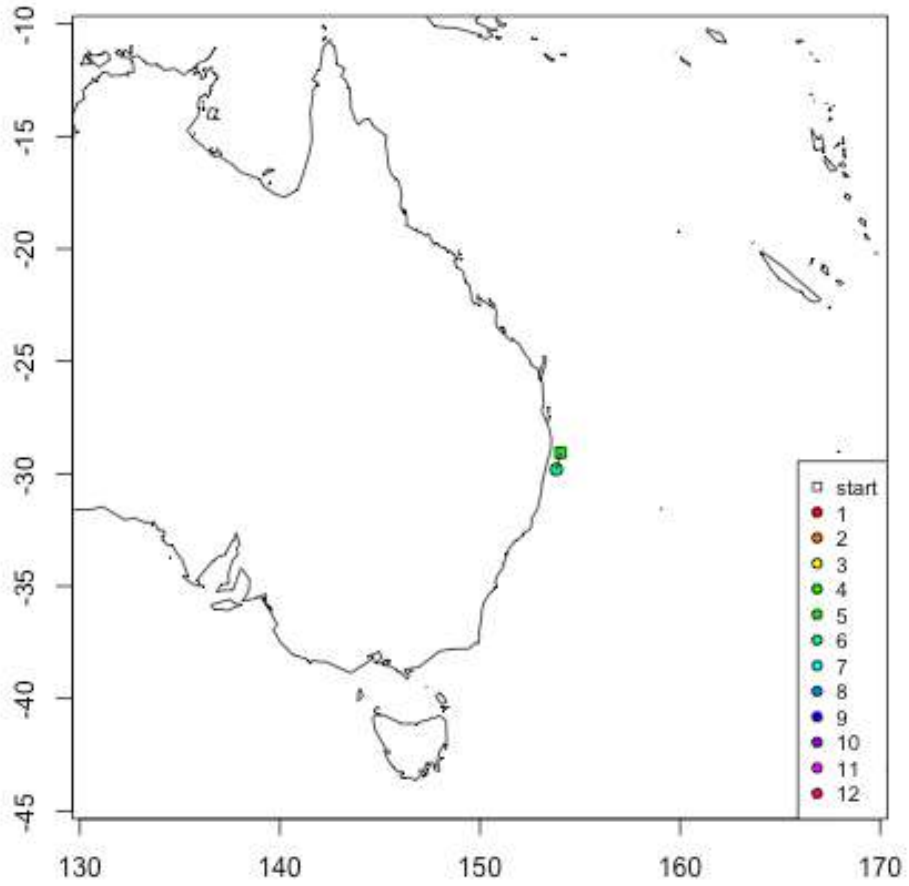

Figure A3. 11. Map of the locations recorded by tag 83864. Legend shows the starting location and all locations recorded by the tag coloured by month.

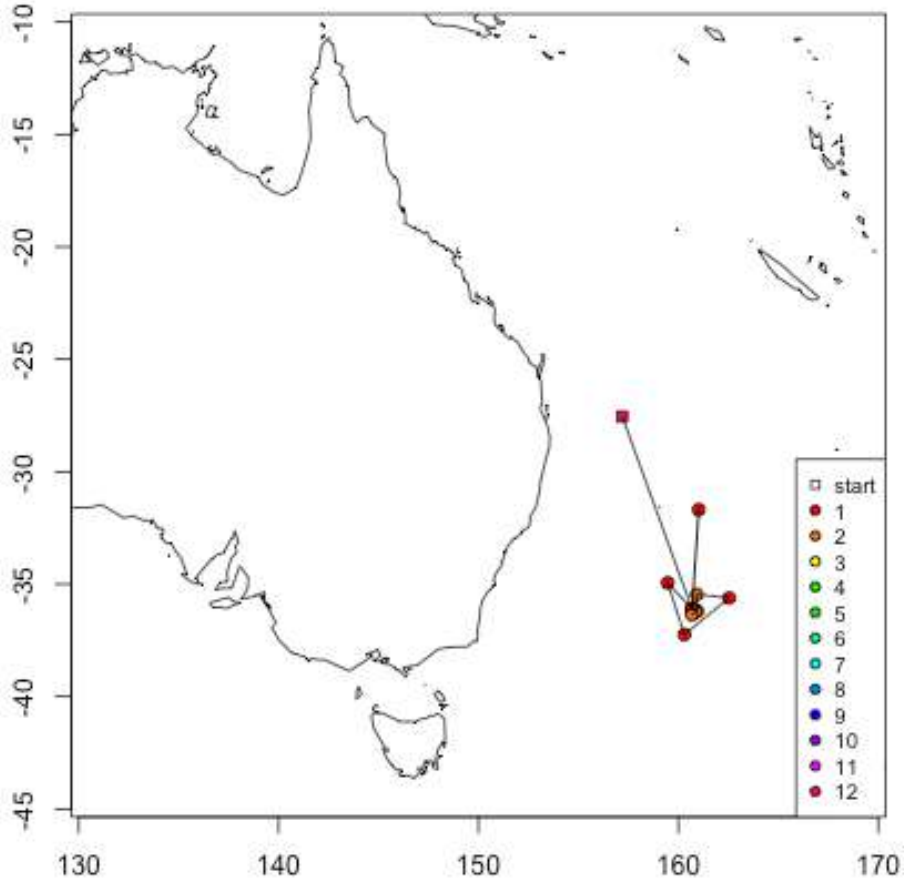

Figure A3. 12. Map of the locations recorded by tag 84184. Legend shows the starting location and all locations recorded by the tag coloured by month.

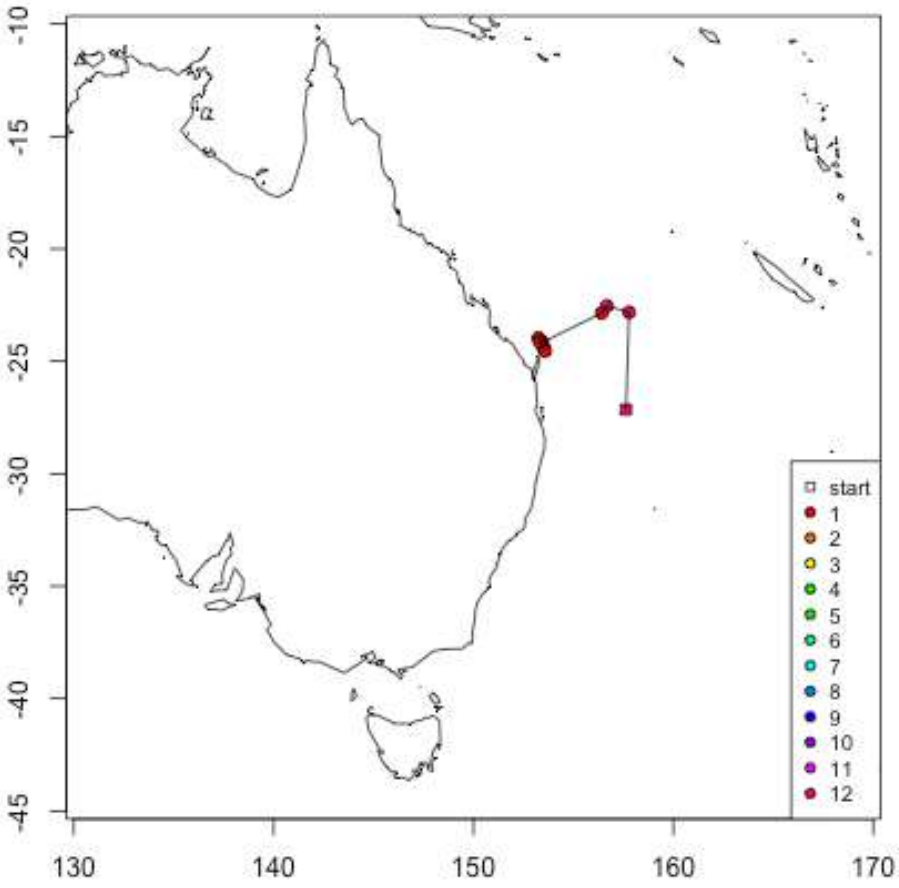

Figure A3. 13. Map of the locations recorded by tag 84186. Legend shows the starting location and all locations recorded by the tag coloured by month.

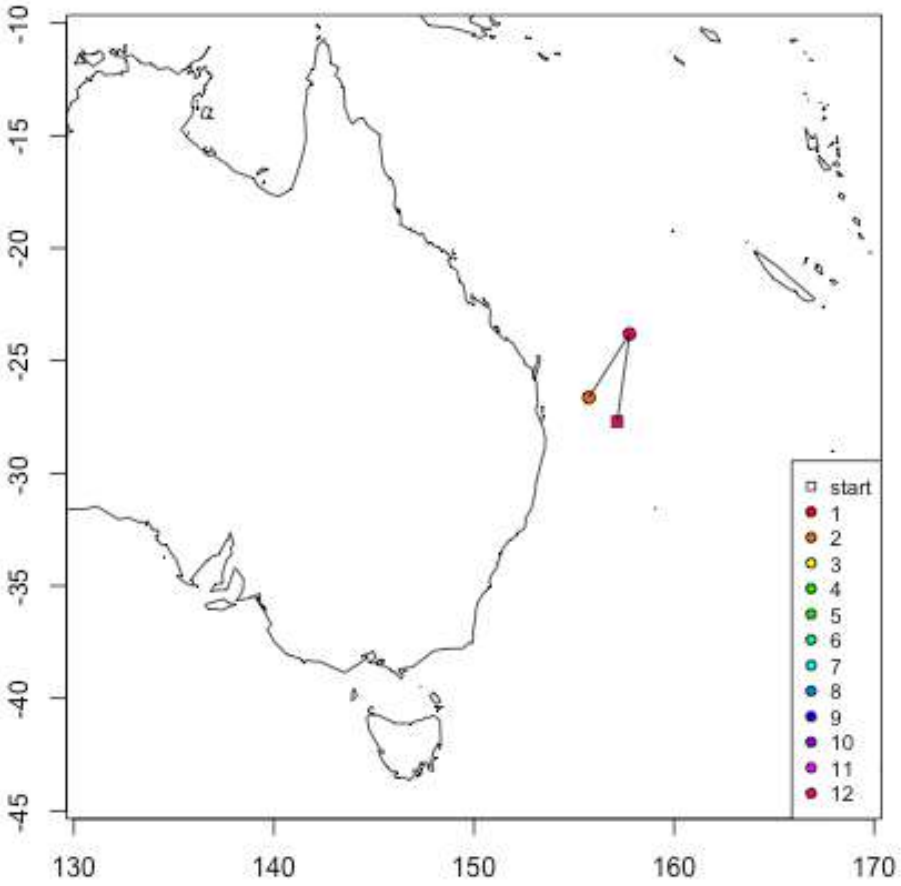

Figure A3. 14. Map of the locations recorded by tag 86588. Legend shows the starting location and all locations recorded by the tag coloured by month.

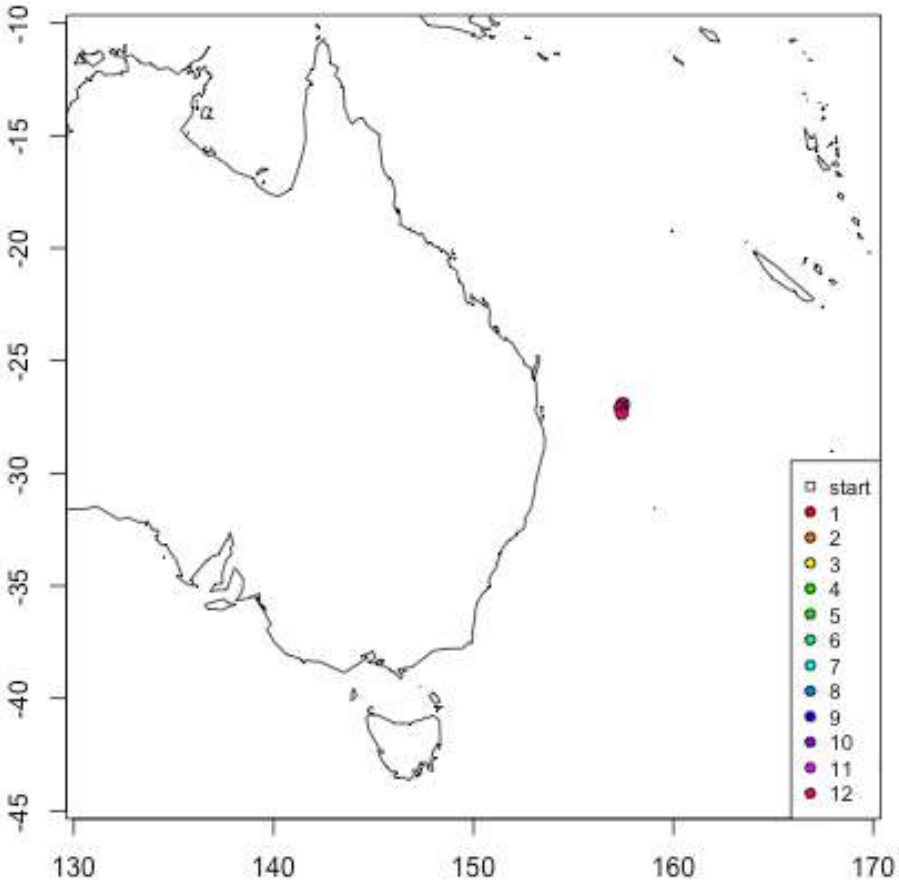

Figure A3. 15. Map of the locations recorded by tag 86589. Legend shows the starting location and all locations recorded by the tag coloured by month.

Table A3.1 Wildlife Computers Mk 10 PSAT data returned by tags used in FRDC project 2007/036

Tag Id	Latitude	Longitude	Residual	Type	Year	Month	Day
36861	-29.36	159.60	0	release	2008	2	28
36861	-28.44	161.08	0	recovery	2008	3	5
37702	-25.98	156.96	0	release	2008	3	23
37702	-24.61	159.34	15811.4	GPS	2008	3	1
37702	-24.61	159.34	18257.4	GPS	2008	3	4
37702	-26.71	159.05	7826.3	GPS	2008	3	8
37702	0.00	0.00	0	GPS	2008	3	18
37702	-25.70	156.70	0.5	GPS	2008	3	20
37702	-25.76	156.57	6.5	GPS	2008	3	22
37702	-24.61	159.34	0.2	GPS	2008	4	8
37702	-24.37	160.94	4.5	GPS	2008	4	14
37702	-24.05	161.44	5.5	GPS	2008	4	16
37702	0.00	0.00	0	GPS	2008	4	20
37702	-23.51	162.26	1.6	GPS	2008	4	21
37702	-23.55	162.20	9.4	GPS	2008	4	22
37702	-23.56	161.84	0	recovery	2008	4	23
39796	-24.75	155.46	0	release	2008	11	6
39796	-16.05	161.10	13355.9	GPS	2008	12	3
39796	-15.92	158.28	15811.4	GPS	2008	12	5
39796	-15.92	158.28	18257.4	GPS	2008	12	8
39796	-15.92	158.28	12909.9	GPS	2008	12	14
39796	-15.92	158.28	15811.4	GPS	2008	12	18
39796	-15.91	158.27	0	recovery	2009	1	4
39969	-25.95	156.82	0	release	2008	3	25
39969	-29.31	160.75	3624	GPS	2008	3	27
39969	-34.70	161.39	3200	GPS	2008	3	29
39969	-34.20	156.21	14142.1	GPS	2008	3	31
39969	0.00	0.00	0	GPS	2008	4	6
39969	0.00	0.00	0	GPS	2008	4	9
39969	-34.20	156.21	15811.4	GPS	2008	4	10

Wildlife Computers Mk 10 PSAT data returned by tags … continued

Tag Id	Latitude	Longitude	Residual	Type	Year	Month	Day
39969	-32.34	153.49	4	GPS	2008	4	16
39969	-34.06	152.76	7.6	GPS	2008	4	18
39969	-33.56	154.38	3460.2	GPS	2008	4	19
39969	-33.22	154.28	7.4	GPS	2008	4	25
39969	-34.49	153.53	1.3	GPS	2008	4	29
39969	-34.19	155.53	4.4	GPS	2008	5	3
39969	-34.20	156.21	0.3	GPS	2008	5	4
39969	-34.44	156.62	6.9	GPS	2008	5	5
39969	-34.83	156.87	2	GPS	2008	5	6
39969	-35.61	156.92	0.2	GPS	2008	5	12
39969	-35.53	155.61	0.6	GPS	2008	5	14
39969	-35.49	155.36	0.2	GPS	2008	5	15
39969	-36.04	153.36	3.2	GPS	2008	5	19
39969	-36.45	151.88	0.1	GPS	2008	5	22
39969	-36.28	151.77	0	recovery	2008	5	23
39970	-25.73	156.09	0	release	2008	12	12
39970	-25.08	156.45	0.7	GPS	2008	12	13
39970	-24.73	156.86	1.5	GPS	2008	12	15
39970	-24.69	157.46	8.8	GPS	2008	12	18
39970	-24.67	157.48	4.8	GPS	2008	12	18
39970	-24.98	160.16	3.9	GPS	2009	1	9
39970	-26.41	158.46	0.2	GPS	2009	1	14
39970	-26.90	158.13	9.7	GPS	2009	1	17
39970	-29.83	156.84	1.9	GPS	2009	1	31
39970	-31.20	156.08	0.6	GPS	2009	2	5
39970	-32.18	155.87	0.2	GPS	2009	2	7
39970	-33.24	156.45	0	recovery	2009	2	9
83860	-25.55	155.65	0	release	2008	11	8
83860	-25.05	156.92	19.5	GPS	2008	11	18
83860	-25.11	156.89	643.4	GPS	2008	11	18

Wildlife Computers Mk 10 PSAT data returned by tags … continued

Tag Id	Latitude	Longitude	Residual	Type	Year	Month	Day
83860	-25.15	157.00	0.2	GPS	2008	11	19
83860	-25.18	157.02	0.2	GPS	2008	11	19
83860	-25.20	157.06	11.1	GPS	2008	11	19
83860	-25.20	157.06	11.1	GPS	2008	11	19
83860	-25.20	157.07	5.4	GPS	2008	11	19
83860	-25.20	157.07	0.8	GPS	2008	11	19
83860	-25.35	157.26	4.4	GPS	2008	11	20
83860	-25.35	157.28	0.7	GPS	2008	11	20
83860	-25.35	157.30	0.2	GPS	2008	11	20
83860	-25.36	157.36	6.9	GPS	2008	11	20
83860	-25.42	157.55	0	recovery	2008	11	21
83861	-25.73	156.24	0	release	2008	12	13
83861	-36.33	160.97	1090.9	GPS	2009	2	2
83861	-32.49	158.72	8.4	GPS	2009	2	9
83861	-32.82	159.24	0	recovery	2009	2	10
83862	-28.71	154.04	0	release	2008	6	19
83862	-21.83	159.06	0	recovery	2008	8	17
83863	-25.89	155.36	0	release	2008	12	15
83863	-36.31	152.32	17651.9	GPS	2008	12	22
83863	-34.54	153.87	15811.4	GPS	2008	12	25
83863	-31.01	153.79	764.8	GPS	2009	1	19
83863	-33.53	152.79	381.5	GPS	2009	1	30
83863	-34.77	153.94	0	recovery	2009	2	12
83864	-29.07	154.03	0	release	2008	5	25
83864	-29.81	153.82	0	recovery	2008	6	2
84184	-27.55	157.19	0	release	2009	12	10
84184	-36.12	160.69	18257.4	GPS	2009	12	24
84184	-36.12	160.69	15811.4	GPS	2009	12	30
84184	-36.12	160.69	15811.4	GPS	2010	1	1
84184	-36.12	160.69	12909.9	GPS	2010	1	2

Wildlife Computers Mk 10 PSAT data returned by tags … continued

Tag Id	Latitude	Longitude	Residual	Type	Year	Month	Day
84184	-31.69	161.02	8630.5	GPS	2010	1	5
84184	-36.12	160.69	15811.4	GPS	2010	1	7
84184	-36.12	160.69	15811.4	GPS	2010	1	8
84184	-36.12	160.69	14142.1	GPS	2010	1	14
84184	-34.94	159.46	1.9	GPS	2010	1	16
84184	-37.24	160.30	15390.2	GPS	2010	1	23
84184	-35.62	162.54	2432.9	GPS	2010	1	27
84184	-35.46	160.92	0.1	GPS	2010	2	3
84184	-36.19	160.95	2.7	GPS	2010	2	4
84184	-36.23	160.89	7.8	GPS	2010	2	5
84184	-36.37	160.68	0	recovery	2010	2	6
84186	-27.15	157.63	0	release	2009	12	7
84186	-22.82	157.79	0.8	GPS	2009	12	24
84186	-22.54	156.68	3.9	GPS	2009	12	29
84186	-22.85	156.42	9.8	GPS	2010	1	1
84186	-24.15	153.45	8.4	GPS	2010	1	15
84186	-23.96	153.25	8.7	GPS	2010	1	21
84186	-24.13	153.30	0.2	GPS	2010	1	22
84186	-24.46	153.54	2	light	2010	1	22
84186	-24.46	153.54	2	light	2010	1	22
84186	-24.54	153.59	0	recovery	2010	1	23
86588	-27.70	157.16	0	release	2009	12	11
86588	-23.81	157.77	2314.8	GPS	2009	12	28
86588	-26.64	155.74	0	recovery	2010	2	17
86589	-26.94	157.47	0	release	2009	12	6
86589	-26.94	157.47	10.1	GPS	2009	12	6
86589	-27.08	157.36	0.6	GPS	2009	12	7
86589	-27.33	157.41	0	recovery	2009	12	8

APPENDIX 4. PARAMETER ESTIMATES FOR ALL FITTED MODELS.

Table A4.1 Statistical estimates for all movement models presented in the report

MODEL AND PARAMETERS	AIC	ESTIMATE	LOWER 95% CI	UPPER 95% CI
$\text{logit}(o_{ij}) = e^{-\alpha D_{ij}}$	1430.0			
$-\alpha$		0.0025	0.0007	0.0043
$\text{logit}(o_{ij}) = \beta_L L_j + e^{-\alpha D_{ij}}$				
2 BLOCK MODEL	1437.9			
β_2		-0.42	-0.42	-0.42
$-\alpha$		-1.1	-2.1	-1.1
4 BLOCK MODEL	1396.0			
β_4		-3.3	-3.4	-3.3

Statistical estimates for all movement models presented in the report…continued

MODEL AND PARAMETERS	AIC	ESTIMATE	LOWER 95% CI	UPPER 95% CI
β_3		12.7	12.7	NA
β_2		20.3	5.7	NA
$-\alpha$		-10.6	NA	NA
8 BLOCK MODEL	1390			
β_8		-2.5	NA	NA
β_7		40.2	NA	NA
β_6		8.3	NA	NA
β_5		-3.0	NA	NA
β_4		-93.1	NA	NA
β_3		31.5	NA	NA

Statistical estimates for all movement models presented in the report…continued

MODEL AND PARAMETERS	AIC	ESTIMATE	LOWER 95% CI	UPPER 95% CI
β_2		32.1	NA	NA
$-\alpha$		-0.0047	NA	NA
$\text{logit}(o_{ij}) = \beta_L L_j + \beta_{SL} L_j S_t + e^{-\alpha D_{ij}}$	1418			
β_2		3.53	NA	NA
β_{12}		-9.72	-15.51	3.93
β_{11}		-5.93	-13.95	2.09
$-\alpha$		-0.002	-0.00108	-0.00292

Statistical estimates for all movement models presented in the report…continued

MODEL AND PARAMETERS	AIC	ESTIMATE	LOWER 95% CI	UPPER 95% CI
$\text{logit}(o_{ijk}) = \beta_\delta \delta_{jk} + e^{-\alpha D_{ij}}$	1263.6			
β_δ		-0.0034	-0.00393	-0.00287
$-\alpha$		-0.0044	0.0012	0.0076

Contact Us
Phone: 1300 363 400
+61 3 9545 2176
Email: enquiries@csiro.au
Web: www.csiro.au

Your CSIRO

Australia is founding its future on science and innovation. Its national science agency, CSIRO, is a powerhouse of ideas, technologies and skills for building prosperity, growth, health and sustainability. It serves governments, industries, business and communities across the nation.